International Journal of Engineering Trends and Technology
ISSN: 2231–5381 / https://doi.org/10.14445/22315381/IJETT-V72I12P134

Volume 72 Issue 12, 397-417, December 2024

Original Article

Reliability Analysis of Unstabilized Rammed Earth Under Seismic Loads using Monte Carlo Simulation

Chaymae Salhi[1], Mouna El Mkhalet[2], Nouzha Lamdouar[3]

[1]*Civil Engineering and Construction structure GCC laboratory, Mohammadia School of Engineers EMI, Mohammed V University, Rabat, Morocco.*
[2]*Mohammadia School of Engineers, Mohammed V University, Morocco.*
[3]*Department of Civil Engineering, Mohammadia School of Engineers, Mohammed V University, Morocco.*

[1]*Corresponding Author : chaymae.salhi@research.emi.ac.ma*

Received: 13 August 2024 Revised: 21 November 2024 Accepted: 03 December 2024 Published: 25 December 2024

Abstract *- Rammed earth is experiencing a resurgence of interest due primarily to its environmental properties. This study analyzes the reliability of unstabilized rammed earth in a one-story building under seismic loads, an aspect never addressed in previous research, focusing on out-of-plane bending moments according to the Moroccan Seismic Regulation for Earth Constructions (RPCTerre 2011) using Monte Carlo simulation. Load and resistance parameters were considered dom variables, with additional parameters varying. A Python code was developed for the simulations. The results provide recommendations on wall dimensions and minimum compressive strength for different seismic zones. These recommendations were compared to existing guidelines with seismic provisions, revealing some commonalities. However, the comparison also highlights suboptimal thickness values for low and low seismicity zones and insufficient compressive strength recommendations. The study concludes that higher seismicity levels and wider walls require greater minimum thicknesses. This study addresses a crucial gap in the literature by offering a probabilistic analysis of rammed earth structures under seismic loads, providing insights to enhance design guidelines and improve the safety and sustainability of earth construction in seismic regions.*

Keywords *- Monte Carlo simulation, Seismic loads, Structural reliability analysis, Unstabilized rammed earth.*

1. Introduction

Rammed Earth (RE) and earthen materials generally experienced a decline with the ascendancy of concrete in the 20th century when concrete became the dominant construction material [1]. However, in recent decades, there has been a renaissance of earthen materials, including RE, in response to the current environmental situation, mainly due to their environmental qualities [2-4]. In this context, many researchers have begun reassessing RE, recognizing it as environmentally responsible and a technique with 'excellent sustainability credentials' [5]. RE has demonstrated lower environmental impacts [6], attributed to its lower embodied energy and carbon footprint when compared to conventional industrial construction materials like concrete, steel or masonry [7] [8] [9]. The technique primarily uses raw earth, which is highly abundant and one of the most predominant materials to avoid dependence on imports [10]. Additionally, RE does not need firing treatment [11] and offers potential for recycling [10]. RE technique consists of compacting earth layer by layer using a temporary formwork removed afterwards, resulting in a monolithic wall [12]. Each layer is 10 to 15 cm thick before compaction and between 6 and 10 cm after [7][8][12]. A manual or pneumatic rammer is utilized to compact earth layers [13]. Earth composition and mixture used vary greatly, but generally, RE employs clayey soil [7] and is compacted to an approximate optimum moisture content [13]. The earth mixtures employed for RE are generally characterized by a poorly sorted particle size distribution balanced between clay, sand and aggregate (up to 64 mm) [14][8]. When clay is the sole binder between grains, it is commonly known as Unstabilized Rammed Earth (URE) [13]. However, when additional binders, including lime or cement, are incorporated, the material is known as stabilized rammed earth SRE [15]. However, RE has not been traditionally considered an ‘engineered construction technique’. As a result, there was no perceived need for building standards before [16]. Rather, it results from empirical optimization and knowledge of the local materials since its inception [7-17]. To this day, comprehensive design and construction codes for RE structures remain limited compared to concrete and steel structures, primarily attributed to the diverse nature of soil composition and the insufficient research on the behavior of RE structures [18]. In regions susceptible to seismic activity, these factors raise a significant cause for concern since their seismic capacity is significantly low [19]. In the field of RE, various studies have investigated

numerous aspects of the subject. A prominent trend in the current body of research is a strong focus on the experimental characterization of mechanical behavior for both URE and SRE. For URE, notable studies include, for instance, [7] that investigated the mechanical properties of URE, including elastic modulus and compressive strength, through dynamic on-site testing, laboratory compression tests, and micromechanical analysis. Their experiments were conducted at three scales: in-situ walls, Representative Volume Elements (RVE) in the laboratory, and Compressed Earth Blocks (CEBs). Another significant study [20], which explored URE's mechanical properties, conducted uniaxial compression tests. They also examined the long-term behavior of URE, including creep behavior under sustained load.

In the realm of SRE, many studies have focused on stabilizers and binders to enhance RE's mechanical behaviour. For example, [21] proposed alternative SRE materials, including industrial by-products and recycled waste, evaluating their durability through various tests. Similarly, [22] explored the mechanical behavior of plain and coir fiber-reinforced cement-stabilized RE under compression, tension, and shear. Additionally, numerical modeling has been a significant focus in RE research. [23] performed a numerical simulation using Drucker-Prager elasto-plastic model to analyze the mechanical behavior of RE under axial and diagonal compression. On the other hand, the study by [24] examined the out-of-plane seismic performance of RE walls through finite element simulations. Regarding seismic assessment, existing studies focused primarily on experimental testing, with the majority evaluating the in-plane seismic performance [25], while out-of-plane loading remains less thoroughly explored [24]. For example, studies such as those by [26][27][28] investigate aspects of seismic behavior.

Among other aspects beyond mechanical and seismic performance, other aspects of RE have been investigated in the literature, such as its hygrothermal properties [29] and [30] and the preservation of traditional RE structures [31] and [32]. In terms of reliability analysis, the literature on RE is sparse. According to the authors' knowledge, the only study that tackled this subject is by Kianfar and Toufigh [33], who utilized the First-Order Reliability Method (FORM) to evaluate the reliability of URE and cement-stabilized RE structures, taking into consideration various loading conditions, such as dead loads, live load, and environmental loads. Given the current landscape, where the limited focus has been directed toward the reliability analysis of RE structures, lacking substantial research addressing seismic load considerations, and with out-of-plane loading remaining understudied, existing studies primarily focus on experiments and numerical modeling. This paper seeks to fill the gaps in the existing literature by addressing the uncertainties surrounding the factors affecting the performance of RE, with specific emphasis on the out-of-plane bending of URE under seismic loads. This research is particularly crucial when considering seismic loading since the previous study on the reliability of RE conducted by [33] did not account for seismic forces.

2. Methods

Among other effects of the lateral forces on RE walls, out-of-plane bending is a significant consideration [34]. This paper focuses on seismic loads as the lateral force acting on URE walls. The URE wall is modeled as a thin plate, supported along its edges, and exposed to uniformly applied seismic forces. Following the RPCTerre [34] guidelines, the limit state function is developed using Lévy's solution within the thin plate theory. The random variables and other parameters identified for analysis were derived from the developed form of the limit state function. These variables include compressive strength, density, dead load, live load and roof live load, alongside parameters such as wall thickness, width and height. The statistical distributions and characteristic values for the aforementioned random variables were determined, and pertinent values for deterministic parameters based on existing literature were established.

In fact, for random variables, the compressive strength, a lognormal distribution was adopted with a Coefficient of Variation (COV) of 35%, and the values considered for assessment were 0.5 MPa, 2MPa and 2.5 MPa. Density and dead load were assigned a normal distribution, with mean values of 1900 kg/m^3 and 1.5 kN/m², respectively. Live load and roof live load were assigned a Gumbel distribution, with maximum values of 2 kN/m² and 1 kN/m², respectively. As for deterministic parameters, the wall thickness values assessed were 0.2, 0.25, 0.3, 0.4, 0.5, and 0.6 m, wall width values were 2.5, 3, 4, and 5.2 m, and the wall height values considered were 2.5, 3, and 4 m.

After defining a threshold for the reliability index of 3.8, MCS was performed using a Python script in the PyCharm environment for 500,000 iterations to ensure accuracy. The results, including the probability of failure, were transferred to a Microsoft Excel file for enhanced visibility. The flowchart in Figure 1 represents the research methodology adopted in this paper. The framework and justification for these assumptions are detailed in the following sections.

3. Results

3.1. Literature Review

3.1.1. Reliability Analysis

Reliability analysis, acknowledged as a potent and extensively developed statistical tool, serves to quantify uncertainties in practical problems and anticipate system performance in diverse industries [35-36]. A key aspect of this analysis involves evaluating system failures and their potential consequences [37].

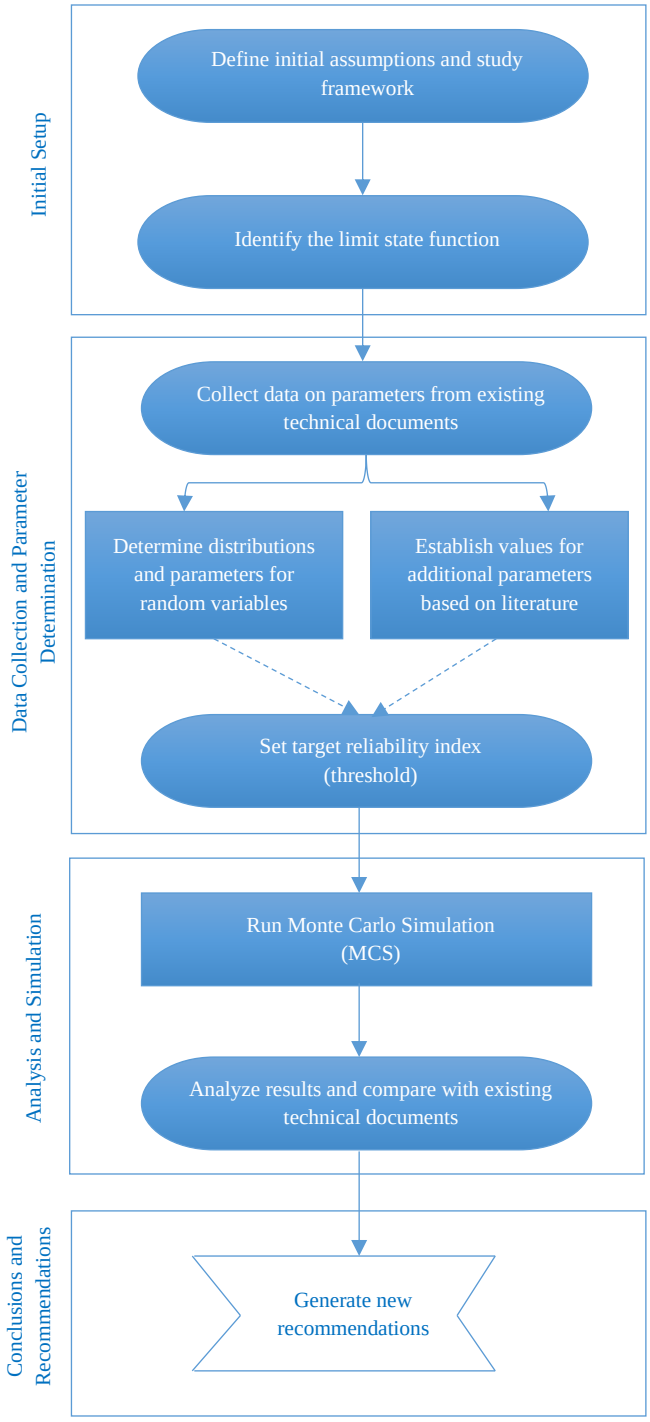

Fig. 1 Research process flowchart

Reliability analysis emerged at the start of the twentieth century and has transformed over the recent decades, transitioning from a specialized field to a prominent topic in many fields [38]. One of the domains in which reliability analysis holds significant prominence is engineering. Notably, numerous studies span a diverse range of engineering domains, encompassing industrial [38-41], aerospace [42, 43], nuclear [44-46], and ocean engineering [47-49].

3.1.2. Structural Reliability Analysis

Inevitably, uncertain elements are present within the production process and the complete lifespan of an engineering structure [50]. Within civil engineering, where uncertainties are integral to factors like resistance parameters and applied loads, as well as their probability of occurrence [33], reliability analysis becomes an indispensable tool for evaluating structural integrity.Structural reliability analysis essentially entails achieving the intended functions, with a significant emphasis on ensuring structural security [50][51] throughout the structure's designed operational lifespan under normal construction and usage circumstances [52]. Structural safety assessment entails accounting for all variations in load and resistance models, analyzing their impact on performance, and calculating the likelihood of failure [51]. In order to accomplish this, it is conventional to consider the limit state function as defined in the following equation in terms of load and resistance [53]:

$$G(X) = R - S \quad (1)$$

R and S denote the overall variables representing structural resistance and load effect, respectively. The failure probability (P_f) can then be obtained using the equation below [53]:

$$P_f = P\{G(X) \leq 0\} \quad (2)$$

Here, the failure and safe regions are denoted as $G(X) \leq 0$and $G(X) > 0$ respectively [53], and the vector $X = [x_1, x_2, \ldots, x_n]$represents the random variables [33]. In the realm of structural reliability methods, both probabilistic and non-probabilistic approaches have reached an advanced level of development, as highlighted by [54].

The complexity inherent in the limit state functions often renders the analytical solution of failure probability integrals challenging [55]. Consequently, researchers and practitioners have focused on developing efficient numerical approaches for approximate solutions, and according to [56], these approaches can be broadly classified into five main groups: stochastic simulation techniques, asymptotic approximation approaches, methods of moments, probability-conservation techniques, and surrogate-based methods.

In the scope of this paper, a focus on probabilistic methodologies is adopted, emphasizing stochastic simulation techniques, particularly MCS, as a specific type of these techniques [55]. In the context of structural reliability analysis for RE structures, the available literature is sparse, with only one study by Kianfar and Toufigh[33].

This study used the FORM to assess the reliability of URE and cement-stabilized RE structures, considering various load and resistance parameters as random variables but did not account for seismic loads, making this paper the first to study the reliability analysis of URE structures considering seismic loads.

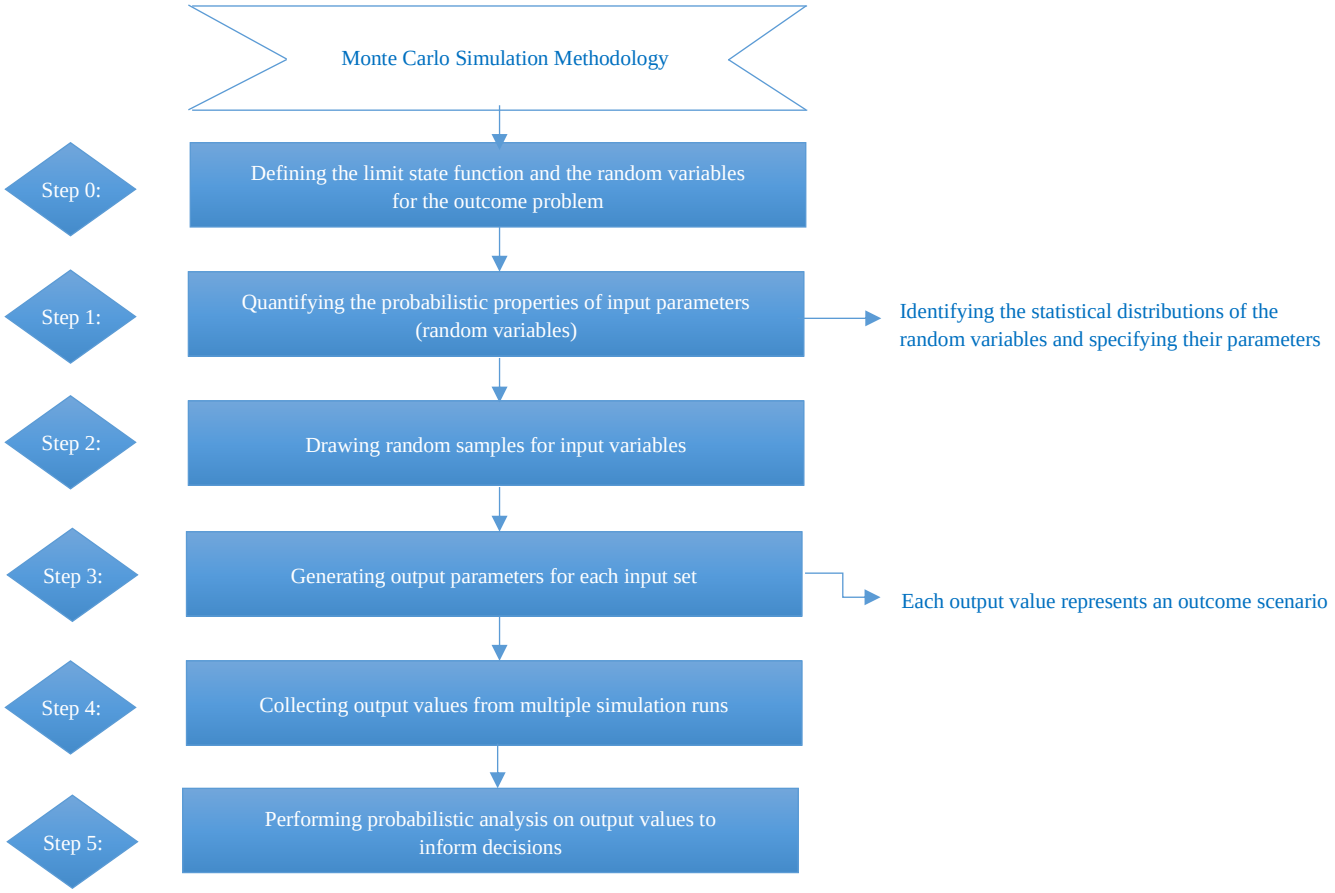

Fig. 2 Flowchart illustrating the steps of the methodology of MCS based on the studies by [56,57]

Table 1. Advantages and drawbacks of the MCS in literature

Advantages	Ref.	Disadvantages	Ref.
Versatile and robust	[50]	Estimating a small failure probability involves high computational expenses	[36]
High accuracy analysis method	[64]	Lacks utility due to its slow convergence	[50]
Can be utilized for various real-world applications, enabling the direct inclusion of any probability distribution type for the random variables	[65]	A significant sample size is required to calculate the probability of failure	[64]
A very appealing simplicity characterizes it	[66]		

3.1.3. Monte Carlo Simulation

MCS relies on iterative random sampling and statistical analysis to generate results for desired outcome problems and to understand the likelihood of an occurrence [55,56]. According to the study by Harrison[57], MCS arose during the Manhattan Project during World War II with John Von Neumann and Stanislaw Ulam, who suggested it in developing nuclear weapons. They, along with others, used simulation to address nuclear weapon challenges and established most of the fundamental methods of MCS [57]. They named the method after the Monte Carlo casino in Monaco due to its reliance on randomness [57]. The Monte Carlo method enables the estimation of the probability of failure, represented as [53]:

$$\overline{P_f} = \frac{N_{fail}}{N_{sim}} \quad (3)$$

Nfail is the total number of failure points, and Nsim is the number of simulations conducted. To illustrate the steps of the MCS, the authors developed a flowchart drawing from the studies by [56,57], as presented in Figure 2.

The advantages and drawbacks of the MCS are presented based on the existing literature in Table 1.

3.2. Case Study

In order to assess the out-of-plane bending of RE walls, the Moroccan Seismic Regulation for Earth Constructions (Règlement Parasismique des Constructions en Terre) [34] suggests the following verification:

$$Mu \leq Mrh = \phi f_{tf} Zu \quad (4)$$

With Mu representing the maximum out-of-plane bending moment due to lateral forces and Mrh representing the resisting moment of the wall. The parameters ϕ, ftf and Zu, refer to the partial safety factor on materials, the flexural tensile strength of the RE wall, and the section modulus of the wall's gross section, respectively.

3.2.1. Initial Assumptions and Framework

Before developing Equation 4, it is crucial to outline the initial assumptions within this framework.

- Lateral Response: In accordance with the specifications of [34], the lateral response of a wall corresponds to that of a plate supported at its edges.
- Plate Categorization: In accordance with [58], plates can be categorized into thin and thick plates. A common criterion for defining thin plates in technical calculations is that the thickness-to-span ratio should not exceed 1/20 when considering the shorter span length [58]. Although some examples of thin plates exist, the prevailing trend in literature and guideline recommendations tends towards considering thick plates. However, to simplify calculations and the problem itself, this paper opts for the theory of thin plates to solve the ultimate out-of-plane bending moment induced by lateral loads.
- Support Condition: In line with the guidelines of [34], which specify edge support for the plate, the URE wall is treated as a supported thin plate.
- Load Distribution: According to Figure 3, sourced from the RPCTerre [34], which depicts the application of lateral forces, the lateral loads are uniformly distributed.
- Loads Considered: It should also be noted that [34] encompasses both seismic and wind loads in the verification of out-of-plane bending due to lateral forces. However, in this paper, exclusive emphasis is placed on seismic loads.

3.2.2. Limit State Function

The research on thin plates is extensive, and the bending of thin plates has been a topic of investigation in solid mechanics for over a century. Additionally, it is a fundamental issue in civil engineering and applied mathematics, with widespread applications [58,59]. Since the fundamental equations and boundary conditions for thin plates were defined long ago, the main interest has shifted toward developing solutions [59]. The analysis of rectangular plates can generally be categorized into two approaches: analytical methods and numerical methods [60]. In the case of static bending of rectangular plates, the governing partial differential equation for the problem proves challenging to solve analytically [59].

Consequently, analytical methods are comparatively scarce, contrasted with the abundance of approximate and numerical techniques [59]. Noteworthy among these are the finite difference method [61], the finite strip method [62], and the Finite Element Method (FEM)[63]. Analytical methods, particularly for plates with supported edges, still rely on foundational solutions like Navier's or Lévy's approaches [60].

In this specific case, dealing with a thin rectangular plate simply supported at its edges under uniformly distributed load, which aligns with a basic plate geometry, specific load configuration, and boundary support conditions, the classic analytical solutions such as Navier's and Lévy's remain pertinent [67].

Based on Table 2, which illustrates the advantages and disadvantages of both methods, the authors judged Lévy's solution to be the most suitable for this case. Based on Lévy's solution and its rapid convergence in most cases, it is sufficient to consider only the initial few terms to ensure accuracy up to the third decimal place [58,68]. Therefore, for a supported rectangular plate, Lévy's solution allows us to suggest the following expression of the maximum out-of-plane bending moments in the plate [58]:

$$Mu_x = \delta_2 p_0 a^2 \quad (5)$$

$$Mu_y = \delta_3 p_0 a^2 \quad (6)$$

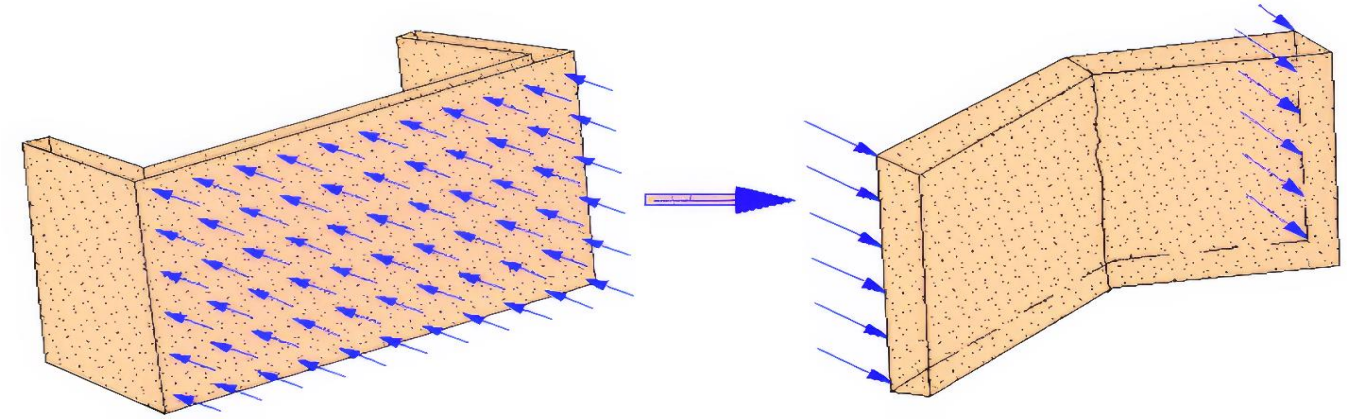

Fig. 3 Out-of-plane bending of a RE wall subjected to seismic forces (*source: [34]*)

Table 2. Advantages and disadvantages of Navier's and Lévy's solutions

Method	Advantages	Ref.	Disadvantages	Ref.
Lévy's Solution	Utilizes a single series, which enhances practicality due to its facilitation of numerical calculations	[58]	The necessary mathematical manipulations may involve considerable complexity.	[68]
	Applicable to plates exhibiting diverse boundary conditions	[67]		
	Convergence remains exceptionally rapid, even in scenarios involving concentrated or line loads.	[68]		
	Given that the solution converges rapidly, in most instances, considering only the initial terms is typically sufficient			
Navier's Solution	It provides considerable mathematical benefits by reducing the solution process from a fourth-order partial differential equation to an algebraic form.	[68]	Employs double series	[58]
			Focused on simply supported rectangular plates within its application context	[68]
			The convergence rate decreases for concentrated and discontinuous loads.	
	Convergence of the series tends to exhibit rapid rates when addressing distributed loads.		The computation of bending moments and shear forces is hindered by the decreased efficiency of the series' convergence.	[67]
			The decreased convergence efficiency is also associated with a loss of accuracy in the calculation process.	

Where p0 is the uniformly distributed static seismic load, a is the width of the URE wall, and δi is determined based on the aspect ratio b/a, with b being the height of the URE wall, as given by [58]. It should be noted that Mux and Muy refer to the maximum out-of-plane bending moment per unit distance along the x-plane and y-plane, respectively. Now, the second term, resisting moment, of Equation 4 is developed. As specified by [34], the flexural tensile strength, in the absence of experimental data, is assumed to be:

$$f_{tf} = 0.1 f_c \quad (7)$$

Here, fc represents the compressive strength.Additionally, [34] suggests that the partial safety factor on materials in the case of seismic calculations should be:

$$\phi = 1 \quad (8)$$

After development, the resisting moment along the x-plane and y-plane, per unit distance, are expressed as:

$$Mrh = Mrh_x = Mrh_y = 0.1 f_c \frac{t^2}{6} \quad (9)$$

Finally, the limit state function for verifying the out-of-plane bending of URE walls, according to the specifications of RPCTerre [34], along the x-plane and y-plane, respectively, is:

$$Gx = \delta_2 p_0 a^2 - 0.1 f_c \frac{t^2}{6} \quad (10)$$

$$Gy = \delta_3 p_0 a^2 - 0.1 f_c \frac{t^2}{6} \quad (11)$$

Before delving into the subsequent sections, it is crucial to highlight, as will be elucidated in the following sections, a notable consistency in constructing buildings with RE walls across various regions worldwide. This observation, coupled with the authors' awareness of the dearth of specific data on the characteristics of RE construction in Morocco, underscores the necessity of deriving values from existing literature. Additionally, all values utilized for random variables and other parameters are summarized and presented in Tables 6, 7 and 8. The selection of random variables detailed in the following section for this study was guided by the sensitivity analysis by Kianfar and Toufigh [33]. In their evaluation of several factors -including compressive strength, erosion ratio, humidity factor, smoothness effect, dead load, density, live load, roof live load, snow CE factor, snow CS factor, snow CT factor, snow ground load, and wind speed- they identified compressive strength, wind speed, and humidity as the most influential variables affecting the reliability of RE structures. Adapting their findings to the context of the limit state function (Equation 10 and Equation 11), compressive strength as a random variable was prioritized due to its significant impact on reliability, as supported by their results. Density, live load, roof live load, and dead load were included to ensure a more diverse analysis. This study excluded wind speed because, as stated in the initial assumptions, lateral loads were limited to seismic loads, and wind loads were not considered. Similarly, humidity was not accounted for in this analysis.

3.2.3. Resistance Random Variables

Compressive Strength

The recommended values for the unconfined compressive strength, as outlined in standards, building codes, and normative documents pertaining to RE with seismic design requirements, as presented in the study by [69], in addition to the minimum value recommended by [34] that were incorporated are provided in Table 3.

Table 3. The recommended mean value of the compressive strength in literature with seismic design provisions

Document ID	Country	Ref.	Recommended values (MPa)
RPCTerre	Morocco	[34]	0.5[a]
NZS 4297:1998	New Zealand	[71]	0.5
HB195-2002	Australia	[72]	0.4-0.6
NMAC 14-7-4:2016	USA	[73]	2.07

[a)]Minimum value recommended

According to [70], the lognormal distribution is the appropriate choice to mathematically represent compressive strength, as it prevents the occurrence of negative values. In the study by Kianfar and Toufigh[33], the authors recommended a minimum compressive strength of 2 MPa for URE. In this context, and based on the data provided in Table 3, this study will assess compressive strengths of 0.5 MPa, 2 MPa, and 2.5 MPa using a lognormal distribution.

3.2.4. Load Random Variables

Density

According to [33], establishing a constant value for material density based solely on aggregates proves challenging. Literature reveals a wide range of density values reported in various studies on URE, ranging from 1750 kg/m³ to 2200 kg/m³ [13]. Drawing on the synthesis of available research, [33] recommend a mean density value of 1900 kg/m³ for RE materials, with a (COV) of 7% and a normal distribution, will be adopted for this study.

Dead Load

The dead load encompasses both the load-bearing wall's weight and the roof's vertical dead loads. The calculation of the load-bearing wall weight necessitates the density, which was previously detailed. Regarding the roof dead loads, [33] derived them from a load of timber floors and tiled roofs, with a mean value of 1.5 kN/m², a COV of 7% and a normal distribution.

This value accounts for the permanent loads typically experienced by a standard timber floor [33]. While some studies have investigated building materials and different layers of RE building roofs, such as the study by [74], precise data on characteristics such as density and thickness for roof layers and the density of earth used in RE walls in the Moroccan context are lacking in the literature. This absence of data complicates the calculation of dead load in this context. Therefore, the authors adopt the aforementioned value for roof dead loads in this paper.

Live Load

Live loads encompass those associated with the occupancy and utilization of the building, including the roof live load. In the study by Kianfar and Toufigh[33], the Gumbel probability distribution was adopted to evaluate live and roof live load. They used a maximum live load of 2 kN/m², a typical value applied in residential areas, with a COV of 29%. Additionally, the French standard NF P 06-001 [75], adopted in the Moroccan context, specifies the live load for residential floors as 1.5 kN/m², consistent with the aforementioned values. According to [33], the maximum roof live load on tiled timber floors was determined to be 1 kN/m², with a COV of 29%. For consistency, this paper will adhere to these values.

Seismic Loads

According to [34], the lateral seismic force in RE walls must be calculated using the following expression:

$$p_0 = SICW \tag{12}$$

S represents the site coefficient, contingent upon the nature of the foundation soil. In this paper, S=1.2 is adopted, as recommended by [34], for cases lacking specific information on soil characteristics, aiming to maintain a broader context. Here, I serve as the importance factor, equal to 1, since this paper primarily focuses on residential buildings, which are considered, according to [34], alongside those used for offices or commercial purposes, as standard constructions with earth. Where C denotes the seismic coefficient, dependent on the Moroccan seismic zone classification. RPCTerre [34] delineates 5 zones, which will be considered to evaluate the seismic aspect comprehensively. Table 4 presents the different seismic coefficient values with the assigned designations to facilitate a clear understanding of the various seismic zones.

When the load W, representing the structural load-bearing capacity, comprises the total permanent loads G and a fraction Ψ of the operational loads Q, contingent on the nature and duration of the loads. It is expressed as follows:

$$W = G + \psi Q = g1 + g2 + \psi(q1 + q2) \tag{13}$$

Where g1 represents the weight of the wall, g2 denotes the dead loads of the roof, q1 signifies the live load for residential floors, and q2 represents the roof's live load.

3.2.5. Other Parameters

Wall Thickness

One of the parameters commonly cited in handbooks and guidelines is the minimum external wall thickness. Table 5 illustrates the various minimum external wall thicknesses for RE walls in publications with seismic provisions, as outlined in the review by Thompson et al. [69], the value recommended by [34] included. The thickness values of the external walls assessed in this study are 0.2m, 0.25m, 0.3m, 0.4m, 0.5m, and 0.6m, based on the data in Table 5.

Table 4. Designations for various seismic coefficient values

Seismic Coefficient C	Designation
0.1	Very low seismicity
0.13	Low seismicity
0.16	Moderate seismicity
0.18	High seismicity
0.2	Very high seismicity

Table 5. Minimum external wall thickness recommended

Document ID	Country	Ref.	Recommended values (m)
RPCTerre	Morocco	[34]	0.4[a]
Arya	Afghanistan	[78]	0.3
HB195-2002	Australia	[72]	0.2
IS 13837:1993	India	[79]	0.3
NBC 204:1994	Nepal	[80]	0.4-0.45
NZS 4297:1998	New Zealand	[71]	0.25-0.35
NMAC 14-7-4:2016	USA	[73]	0.457

[a)]In [34], the recommendation is not explicitly specified for external walls; instead, it is presented as a general recommendation

Height of URE walls

In Australia, typical residential buildings have RE walls with a height of 2.4 m [76]. In Morocco, based on the study by Baglioni et al.[74], wall heights vary widely from 2.5 to 5 m. Traditional buildings in France and Colombia typically feature RE walls with a height of 3 m [19,77]. Accordingly, across various regions worldwide, the literature reports wall heights for URE ranging from 2.4 to 5 m for both traditional and contemporary buildings. However, in the seismic context following the recommendations of [34], the wall height for single story buildings is constrained to 4 m. Therefore, heights exceeding 4 m in the case of a one-story building are disregarded in this study. Consequently, the URE wall heights evaluated are 2.5 m and 3 m, representing common values used in various contexts and 4 m as the maximum value.

Width of URE walls

According to [77], the width of RE walls in France ranges from 3 to 4.5 m. Reference [24] reported a main RE wall width of 3.6 m in their investigation. Based on a survey of eleven representative RE buildings in southern Portugal, conducted by [81], revealed wall width between 2.2 m and 5.2 m. In accordance with [82], bearing RE walls have widths greater than or equal to 2.5 m. Considering all of this, this paper will consider a minimum width of 2.5 m and a maximum width of 5.2 m, with additional widths of 3 m and 4 m.

3.2.6. Target Reliability Index

The failure probability is related to the reliability index through the following equation [83]:

$$P_f = \Phi(-\beta) \quad (14)$$

Where Φ is the standard normal cumulative density function [33]. According to [33], reliability analysis aims to ensure that the system's failure probability remains below the target threshold or that the reliability index remains above the defined target value In the context of this paper, to the authors' knowledge, there are currently no proposed limits for the target reliability of RE structures, either generally or under seismic loads. Therefore, a target reliability index (TRI) of 3.8, as recommended by [84] for unreinforced masonry structures, will be used in this study. In cases where the probability of failure is 0, a value of 10^{-6}, corresponding to a reliability index of 5.61, was assigned to the probability of failure to ensure clear visualization of the values. This study will focus on comparing different reliability indices for various scenarios to provide new recommendations and verify the recommendations of existing standards. This will serve as an initial basis, pending further studies to establish an accurate target reliability index for RE structures.

3.2.7. Number of Iterations of the MCS

According to [85], a very good estimate value could be achieved in most cases by iterating a simulation anywhere between 100,000 to 500,000 times. Therefore, in this paper, 500,000 iterations were conducted.

3.3. Application

A representative subset of the simulation data generated using Python code is presented before delving into the analysis and discussion of the MCS results for one-story URE walls subjected to seismic loads. For each thickness, height and width combination, the simulation performed 500,000 iterations per seismic coefficient value. This results in 2,500,000 data points per combination, making it impractical to display all results. Table 9 showcases a subset of the results for a specific case of wall thickness t=0.5m, width a=2.5m, height b=3m and compressive f=2MPa. Since Microsoft Excel cannot process 2,500,000 data points per sheet, only 1000 iterations were used in the subset of Table 9 to reduce the simulation time. Reducing the number of iterations decreases the precision of the results [85]. Consequently, the outcomes in Table 9 differ from those obtained with 500,000 iterations. For the same case with 500,000, the probability of failure and the reliability index are respectively Pfx=Pfy=0.002 % and βx=βy=4.16.

3.4. Code Validation Process

The implementation was validated through a Python-based unit testing framework utilizing the *unit test* module. The validation process consisted of three phases:

- Unit Testing of Random Variable Generators: This phase ensured that the random variable generators produced values with the correct statistical properties, adhering to the specified distributions (normal, Gumbel and lognormal).
- Integration Testing: This phase evaluated the combined functionality of multiple components to ensure correct overall performance.

- Accuracy Testing: The final phase verified that the limit state function outputs were computed accurately.

3.4.1. Unit Testing of Random Variable Generators
Normal Distribution

To validate the random value generation for the normal distribution that was employed to represent the dead load G and the material density ρ, the empirical rule for normal distributions [86] was applied. According to this rule, for a dataset with mean $\bar{x}$ and standard deviation s, approximately 68% of the observations lie within $\bar{x}\pm s$, approximately 95% lie within $\bar{x}\pm 2s$ and approximately 99.7% lie within $\bar{x}+3s$. The test confirmed that the generated values adhered to these statistical properties, validating that the random variable generator for normal distribution is accurate.

Gumbel Distribution

For the Gumbel distribution, used for live loads q1 and roof live loads q2, the following aspects were verified:

- The random variables generated by the code were within the expected range.
- The distribution's location (μ) and scale (σ) parameters were calculated correctly.

This validation involved manually calculating the location and scale parameters (μ, β) for both live loads q1 and roof live loads q2, incorporating these values into the test code, and subsequently estimating the parameters within the code using the maximum likelihood method (ML) based on the generated random values, using the following formulas [87]:

$$\beta = \bar{x} - \frac{\sum_{i=1}^{n} x_i \times e^{-\frac{x_i}{\beta}}}{\sum_{i=1}^{n} e^{-\frac{x_i}{\beta}}} \quad (15)$$

$$\mu = \beta\left[ln(n) - ln(\sum_{i=1}^{n} e^{-\frac{x_i}{\beta}})\right] \quad (16)$$

Where $\bar{x} = \sum_{i=1}^{n} \frac{x_i}{n}$ represents the sample mean, and n denotes the sample size. In the python test, the scale parameter β was estimated using an iterative method, Equation 15, with a tolerance of 10^{-6}. Once the value converged, it was substituted into Equation 16 to compute the location parameter μ. The estimated values were then compared with the manually calculated values, and the results matched, confirming that the random samples accurately followed the Gumbel distribution.

Lognormal Distribution

For the lognormal distribution, used for compressive strength fc, the accuracy of the random value generation was validated by verifying the following aspects:

- The random variables generated by the code were within the expected range.
- The distribution's mean (μ) and variance (σ^2) parameters were calculated correctly.

The process involved calculating the mean μ and variance σ^2 of the underlying normal distribution, which are parameters for the lognormal function in Python's *numpy.random.lognormal* [88]. Random values were then generated following the lognormal distribution. The manually calculated mean and variance of the generated samples were computed and compared with the theoretical mean and variance of the lognormal distribution, which were computed using the following equations [89]:

$$\hat{\mu} = e^{\left(\mu+\frac{1}{2}\sigma^2\right)} \quad (17)$$

$$\hat{\sigma}^2 = (e^{\sigma^2} - 1)e^{2\mu+\sigma^2} \quad (18)$$

Where μ and σ^2 represent the mean and variance of the underlying normal distribution, respectively, and $\hat{\mu}$and $\hat{\sigma}^2$ denote the theoretical mean and variance of the lognormal distribution, respectively.The manually calculated and theoretical values were found to be identical, confirming that the lognormal random variable generator is accurate.

3.4.2. Integration Testing

Integration testing involved running the script for every combination of thickness t, width a, height b and seismic coefficient C, for 1000 iterations to minimize computational time. The resulting probabilities of failure Pf_x and Pf_y were verified to lie within the expected range (between 0 and 100). This test confirmed that the combined functionality of all components operated as intended.

3.4.3. Accuracy Testing

The final step validated the accuracy of the limit state function outputs Gx and Gy. Since the accuracy of random value generation had already been tested, the random values for 1000 iterations, as shown in Table 9, were used to calculate the results analytically using the limit state function (Equation 10 and Equation 11). The results were identical, further validating the accuracy.

Note: All testing code and implementation details are provided in the Appendix.

4. Discussion

Prior to analyzing specific cases, an overview of the reliability index results reveals two distinct scenarios: βx=βy and βx≠βy. These scenarios are directly related to the aspect ratio, defined as b/a, where a is the width and b is the height.When the aspect ratio b/a ≤ 1.5, including the cases where a=b, the limit state function in the x and y directions (Gx an Gy) are equal. This equality rises because Gx and Gy differ in their respective values of δi, which are influenced by the aspect ratio b/a [58]. Specifically, when b/a≤1.5, δ2= δ3, resulting in equal reliability indices for both directions (βx=βy). Conversely, the only case where βx≠βy is observed is when the width a=2.5m and the height b=4m, as this configuration yields an aspect ratio b/a>1.5. In the following

sub-sections, after examining the special case where $\beta x \neq \beta y$, the analysis will focus on studying the impact of each variable, whether random or deterministic, on the variation of the reliability index. Given the many variables involved, this approach comprehensively explains how each factor influences the reliability index.

Table 6. Resistance random variables considered

Random variables	Distribution	Values considered	COV (%)
Compressive strength fc (MPa)	Lognormal	0.5	35
		2	
		2.5	

Table 7. Load random variables considered

Random variables	Distribution	Mean value	Max. value	COV (%)	Standard deviation
Density ρ (kg/m^3)	Normal	1900	-	7	133
Dead load G (kN/m²)	Normal	1.5	-	7	0.105
Live load q1 (kN/m²)	Gumbel	-	2	29	-
Roof live load q2 (kN/m²)	Gumbel	-	1	29	-

Table 8. Wall thickness, width and height values are considered

Other parameters	Values assessed (m)					
Wall thickness t	0.2	0.25	0.3	0.4	0.5	0.6
Wall width a			2.5	3	4	5.2
Wall height b				2.5	3	4

Table 9. Subset of results from the MCS run (t=0.2 m| a=3 m |b=2.5 m|f_c=2 MPa)

Seismic Coefficient	Random Variables					Limit state function (MN.m/m)		Failure probability (%)		Reliability Index	
C	G (kN/m²)	ρ (kg/m^3)	fc (MPa)	q1 (kN/m²)	q2 (kN/m²)	Gx	Gy	Pf_x	Pf_y	β_x	β_y
0,1	1,5165	1761,64	1,632	1,192	1,110	-0,0008	-0,0008	0,1	0,1	3,09	3,09
0,1	1,5229	1988,594	1,366	1,056	0,658	-0,00061	-0,00061	0,1	0,1	3,09	3,09
0,1	1,5749	1889,223	2,537	1,134	0,445	-0,0014	-0,0014	0,1	0,1	3,09	3,09
0,1	1,5425	1930,639	2,669	1,319	0,930	-0,00148	-0,00148	0,1	0,1	3,09	3,09
0,1	1,596	2038,134	2,075	1,174	0,636	-0,00107	-0,00107	0,1	0,1	3,09	3,09
0,1	1,6035	1914,075	1,632	1,057	0,368	-0,00079	-0,00079	0,1	0,1	3,09	3,09
0,1	1,4522	2034,452	2,883	0,741	0,326	-0,00163	-0,00163	0,1	0,1	3,09	3,09
0,1	1,5033	1933,71	1,916	1,245	0,329	-0,00098	-0,00098	0,1	0,1	3,09	3,09
0,1	1,4203	1965,177	2,258	1,625	0,411	-0,00121	-0,00121	0,1	0,1	3,09	3,09
0,1	1,4383	1664,318	1,669	0,764	0,645	-0,00085	-0,00085	0,1	0,1	3,09	3,09
0,1	1,4837	1852,633	1,418	1,102	0,602	-0,00066	-0,00066	0,1	0,1	3,09	3,09
0,1	1,3091	1874,74	2,864	1,162	0,503	-0,00163	-0,00163	0,1	0,1	3,09	3,09
0,1	1,6102	1882,39	1,921	0,752	0,662	-0,00099	-0,00099	0,1	0,1	3,09	3,09
0,1	1,5586	1732,291	1,595	1,268	0,815	-0,00078	-0,00078	0,1	0,1	3,09	3,09
0,1	1,3959	1955,276	2,745	0,738	0,606	-0,00154	-0,00154	0,1	0,1	3,09	3,09
0,1	1,3479	2004,202	1,664	1,366	1,293	-0,0008	-0,0008	0,1	0,1	3,09	3,09
0,1	1,4718	1934,26	2,578	1,499	0,562	-0,00142	-0,00142	0,1	0,1	3,09	3,09
0,1	1,3086	1752,929	2,420	1,486	0,382	-0,00135	-0,00135	0,1	0,1	3,09	3,09
0,1	1,6023	2068,243	3,249	1,097	0,472	-0,00185	-0,00185	0,1	0,1	3,09	3,09
0,1	1,5483	1997,831	1,937	1,352	0,419	-0,00099	-0,00099	0,1	0,1	3,09	3,09
0,1	1,3753	1824,2	1,903	0,791	0,974	-0,00099	-0,00099	0,1	0,1	3,09	3,09
0,1	1,6356	2108,684	2,974	0,762	0,531	-0,00167	-0,00167	0,1	0,1	3,09	3,09
0,1	1,54	1728,581	1,008	0,956	0,920	-0,00039	-0,00039	0,1	0,1	3,09	3,09
0,1	1,404	1886,834	1,831	0,770	0,841	-0,00094	-0,00094	0,1	0,1	3,09	3,09
0,1	1,5293	1830,962	2,977	1,158	0,832	-0,0017	-0,0017	0,1	0,1	3,09	3,09
0,1	1,4673	1937,793	2,378	1,084	0,414	-0,00129	-0,00129	0,1	0,1	3,09	3,09
0,1	1,5298	1663,101	2,292	0,750	0,582	-0,00126	-0,00126	0,1	0,1	3,09	3,09
0,1	1,5317	1771,053	1,848	1,248	0,652	-0,00095	-0,00095	0,1	0,1	3,09	3,09

4.1. The case of βx≠βy

In this section, the results of the different values of the reliability index in the case of βx≠βy are presented, considering different thickness values t, alongside fixed parameters C=0.16 (moderate seismicity) and fc=2 MPa (Figure 4). Although eventually βx and βy reach the TRI and for t=0.5m and t=0.6 m, the probability of failure is 0% across all cases, in a broader context, βx<βy. This observation is consistent with expectations and one of the remarks of [58], as a greater height requires less force to achieve ultimate deflection, suggesting that the out-of-plane bending moment along the x-plane Mx is likely greater than My. Given equal resisting moments along both x and y directions, the reliability index associated with the x-axis is lower than that of the y-axis. Furthermore, upon examining the variation of the reliability index with different thickness values, a direct correlation is noted where higher thickness values correspond to higher reliability indices. And despite β_y reaching the TRI across all thickness variations, the disparity in the reliability indices along the x and y directions poses risks, potentially leafing to unpredictability, among other complications. Consequently, it is recommended that such scenarios be excluded from consideration. It is thus recommended that the height b and width a satisfy b/a≤1.5.

4.2. The Impact of the Seismic Coefficient C on the Reliability Index

As previously discussed, the parameter C correlates with seismic zones; higher C values indicate a transition from a lower to a higher seismic zone. It is noteworthy that the reliability index consistently decreases as C values increase, indicating that for the exact wall dimensions and characteristics, higher seismicity zones result in lower reliability. To illustrate this, the examples of a=2.5m, b=3m and fc=0.5 MPa are considered. As shown in Figure 5, the clustered column graph demonstrates the detrimental impact of increasing the seismic coefficient on the reliability index.

This pattern extends to all other cases involving different compressive strengths, widths and heights, which are not depicted in this paper due to space constraints, but all the results will be displayed in the appendix.

4.3. The Impact of the Compressive Strength fc and Thickness t on the Reliability Index

The two possible cases of a=b and a≠b will be showcased to examine various aspects rigorously and determine the consistency of the results across all scenarios.

4.3.1. The case of a=b

In this section, the impact of varying fc under the condition of equal height and width a=b is analyzed. The clustered column graph in Figure 6 illustrates this scenario across different values of compressive strength fc, maintaining a constant seismic coefficient C=0.1 (very high seismicity zone) and thickness t=0.25m. Figure 6 demonstrates how increasing the compressive strength enhances the reliability index. A significant improvement from 0.5 MPa to 2 MPa and 2.5 MPa is observed. The value fc=0.5 MPa demonstrates limited applicability for achieving the reliability threshold fixed since it meets or surpasses the TRI only in specific scenarios, such as for t=0.4 m with certain configurations in very low seismicity zones (C=0.1) and for t=0.5 m and t=0.6 m in very low to moderate seismicity zones (C=0.1, C=0.13 and C=0.16), depending on the dimensions a and b.

However, its performance is highly constrained, requiring thicker walls and low seismic conditions. This observation leads the authors to conclude that 0.5 MPa is not recommended as minimum compressive strength. Instead, 2 MPa is optimal in this study, considering the limit state function used and verification against seismic loads. This conclusion is consistent with the results of [33], who recommends a minimum compressive strength for URE of 2 MPa.

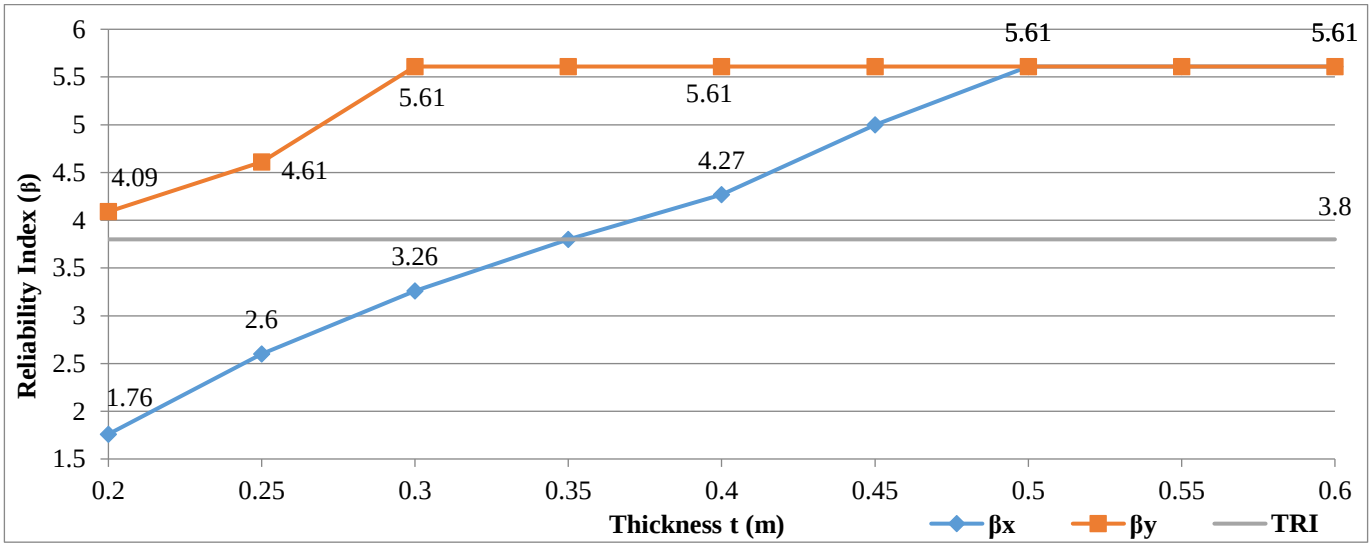

Fig. 4 Reliability index at various thickness values in the case of a=2.5m and b=4m (C=0.16 | fc=2 MPa)

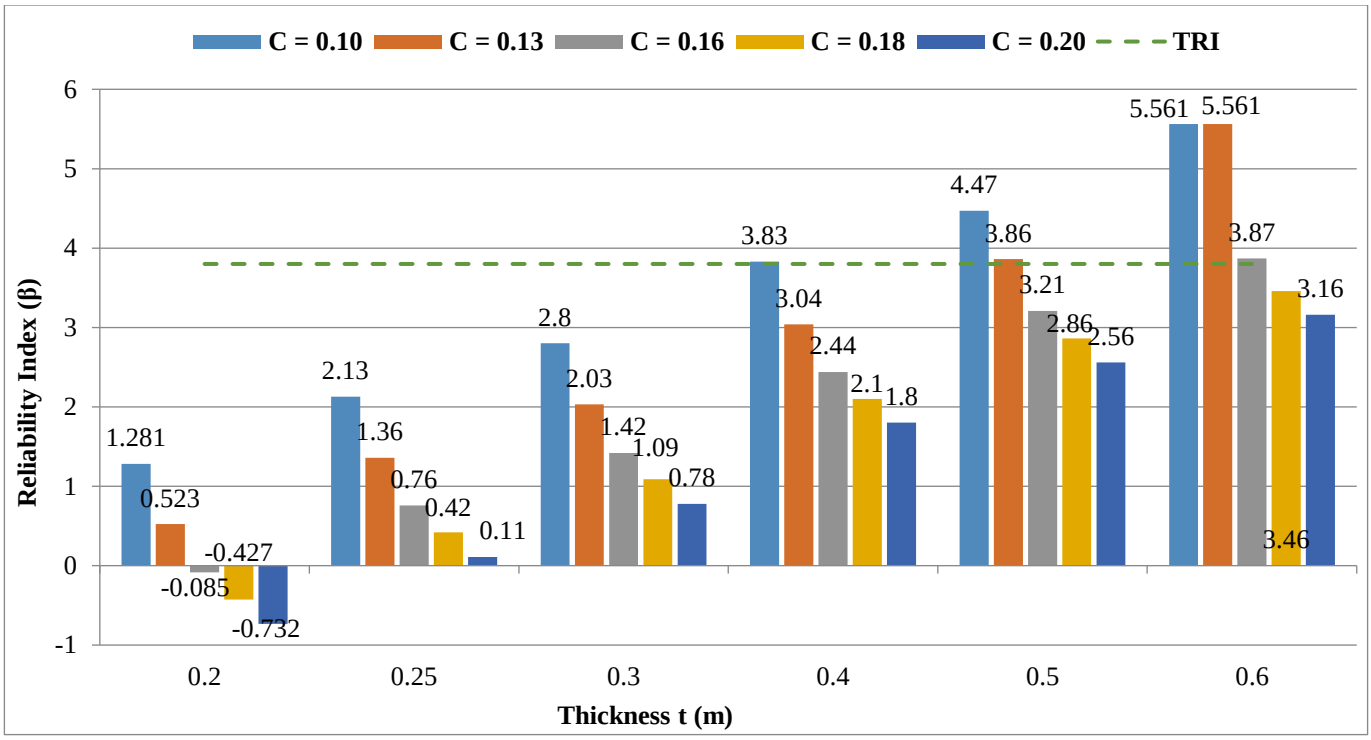

Fig. 5 Reliability index at various seismic coefficient and thickness values (fc=0.5 MPa | a=2.5 m | b=3 m)

Furthermore, Figure 6 shows that increasing the width and height decreases the reliability index. In fact, across all compressive strength values, higher values of a=b correspond to lower reliability indices. Based on Figure 6, the configuration a=b=4 m demonstrates lower reliability results, exceeding the TRI only for fc=2.5 MPa. Across all cases, a width and height of 4 m meets or surpasses the TRI only under specific conditions. For fc=0.5 MPa, it never achieves the TRI. For fc=2 MPa, thicker walls (t ≥0.3 m) and low seismicity zones are required. For fc=2.5 MPa, it performs better, achieving the TRI with thinner walls (t ≥ 0.25 m) in very low seismicity zones and meeting the TRI across all seismic zones for t ≥0.5 m. However, configurations with a=b=2.5 m and a=b=3 m consistently outperform a=b=4 m, achieving the TRI with thinner walls under broader conditions, making them more suitable and practical for design structure. Therefore, the authors do not recommend using a=b=4 m, as it presents higher risks and is significantly more limited in applicability in general.

4.3.2. The case of a≠b

The clustered bar graph in Figure 7 aims to capture the effect of varying thickness and compressive strength on the reliability index. It visualizes the scenario where a=2.5 m and b=3 m across all thickness and compressive strength values in a very high seismicity zone (C=0.2). Figure 7 illustrates the variation of the reliability index with changes in wall thickness and seismic zones, specifically for the case of fc=2 MPa, a=3 m and b=2.5 m. The results for a≠b are consistent with the case of a=b: The reliability index improves with increasing compressive strength. Notably, besides fc=0.5 MPa, as shown in Figure 6, the reliability index remains below the target, reinforcing the observations made in the previous section. In contrast, fc=2 MPa reaches and surpasses the target at t=0.25 m, while fc=2.5 MPa meets and exceeds the TRI across all thickness values in the illustrated scenario. Figures 7 and 8 further demonstrate that higher thickness values enhance the reliability index. Figure 8 shows that t=0.2 m and t=0.25 m yield the lowest reliability indices across all seismic zones, except in the very low seismicity zone (C=0.1). The overall analysis shows that these thicknesses can only meet or exceed the TRI under specific conditions. While performance improves slightly for compressive strength of 2.5 MPa, in the case of 2 MPa- which remains the optimal compressive strength for the studied framework- these thicknesses achieve the TRI for a =2.5m and a=3 m across all wall heights. However, they fail to meet the TRI for all other conditions. And while t=0.25 m performs better, exceeding the TRI in all seismic zones for a=2.5m, both thicknesses remain limited in their applicability. Their overall performance is insufficient, and they represent significant safety risks, especially in the context of seismic evaluations. Hence, the authors do not recommend t=0.2 m and t=0.25 m for URE walls.

4.4. The Impact of Height b on the Reliability Index

To assess the impact of varying heights on the reliability index, the clustered bar graph in Figure 9 is presented. This graph displays the reliability index for all seismic coefficient values with a constant value of the compressive strength fc=2 MPa, thickness t=0.3m, and width a=4m while varying the height b.

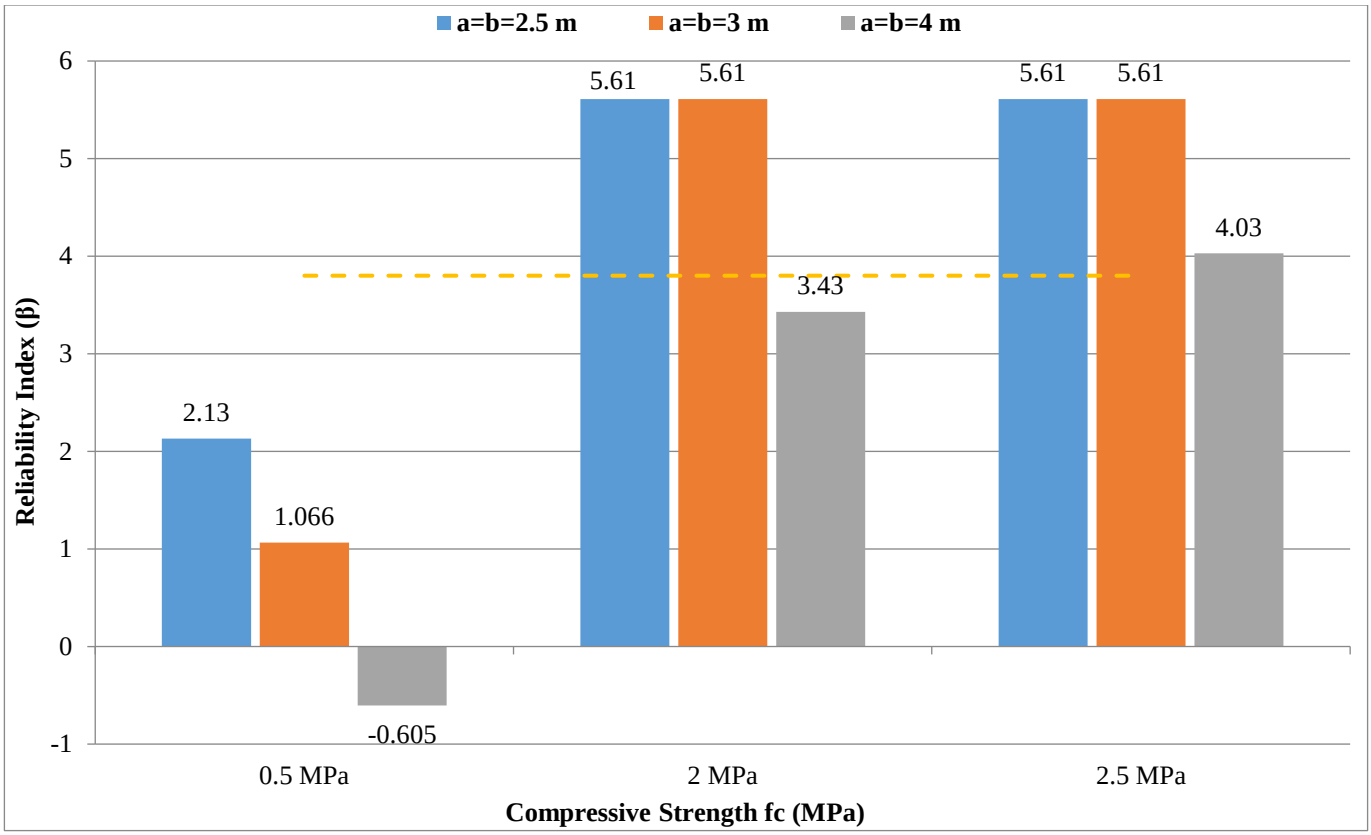

Fig. 6 Reliability index at various compressive strength values: The case of a=b (C=0.1 | t=0.25 MPa)

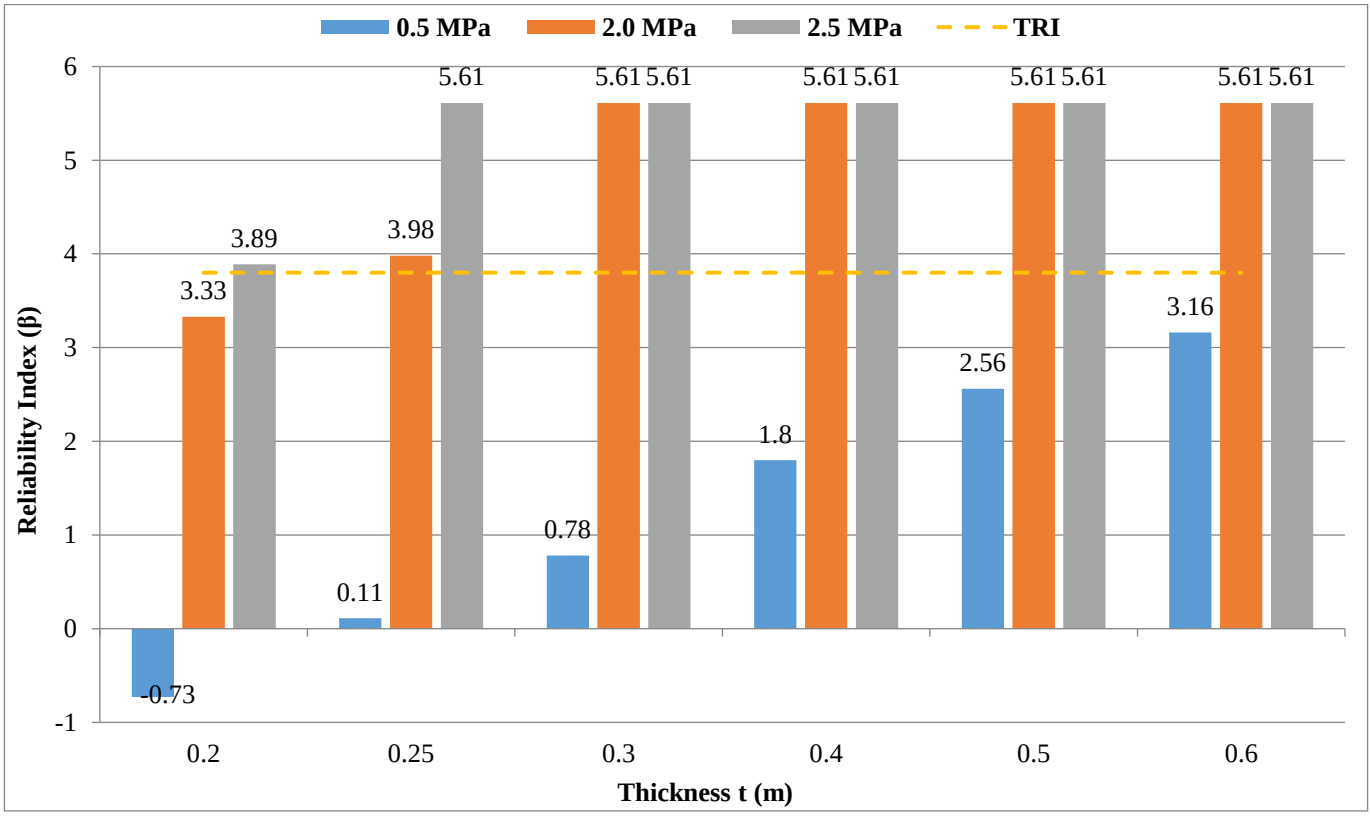

Fig. 7 Reliability index at various compressive strength and thickness values: The case of a≠b (C=0.2 | a=2.5 m | b=3 m)

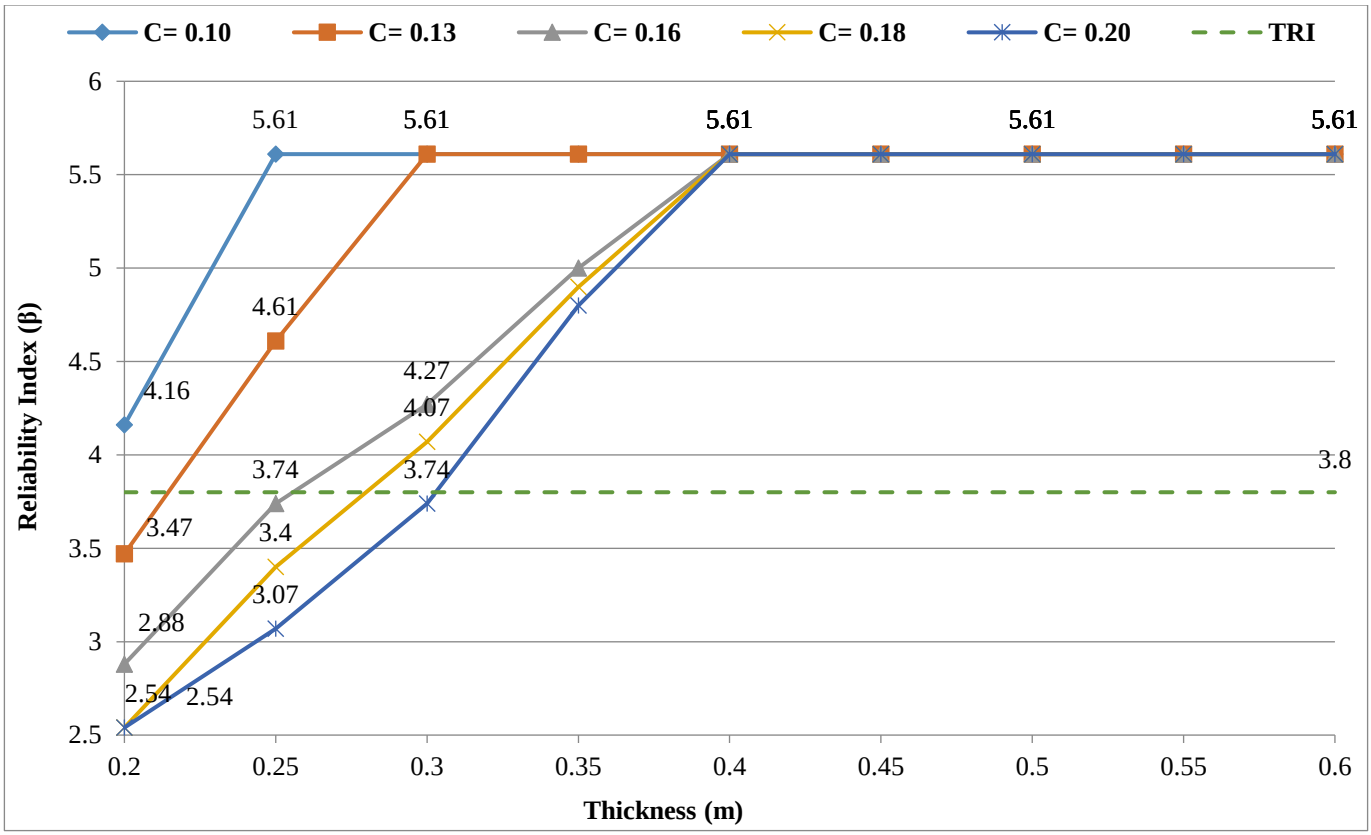

Fig. 8 Reliability index with varying thickness across all seismic zones (fc=2 MPa | a=3 m | b=2.5 m)

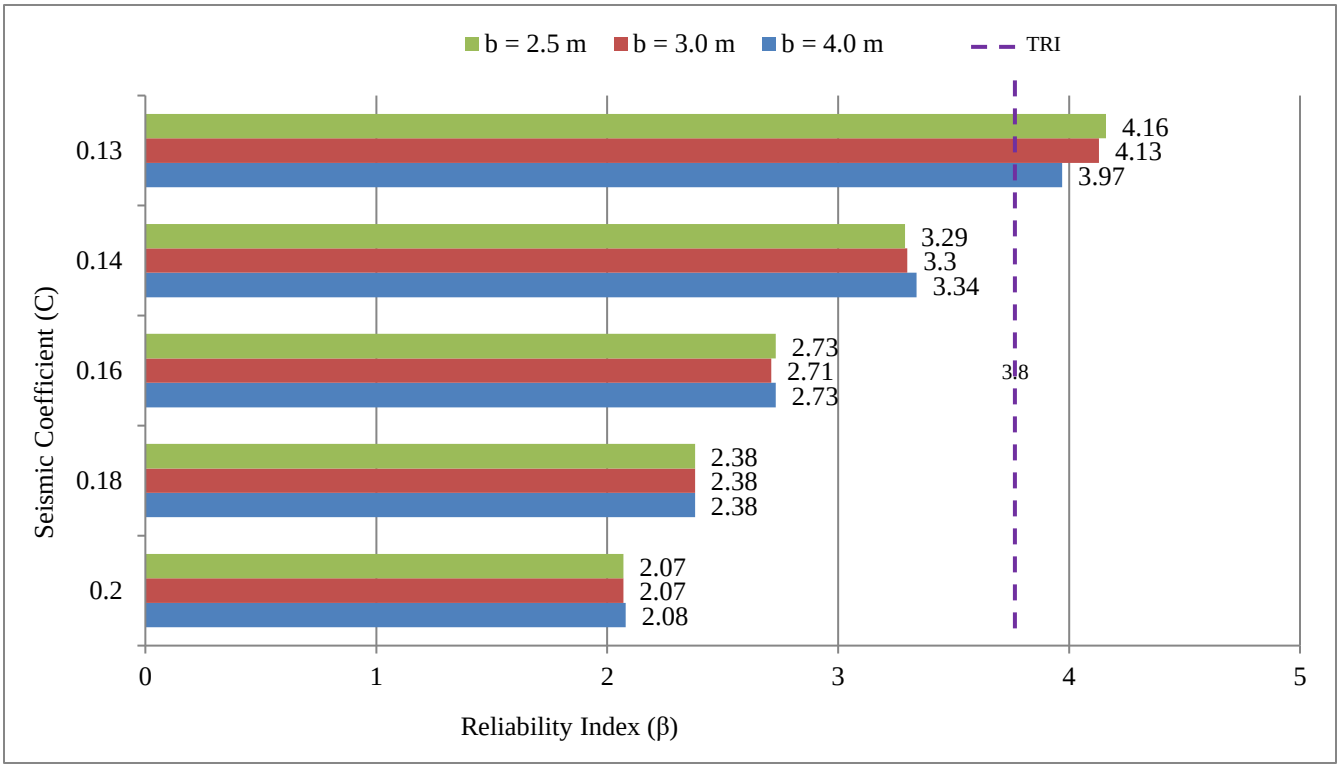

Fig. 9 Reliability index for varying height across all seismic coefficient values (a=4 m | f_c=2 MPa | t=0.3 m)

Figure 9 demonstrates that varying the wall height b does not significantly impact the reliability index values, resulting in similar reliability index values for a constant seismic coefficient across all height values. Additionally, the results are consistent with the previous section, showing that the reliability index decreases with transitioning from a lower seismicity zone to a higher one.

4.5. The Impact of the Width on the Reliability Index

The graph in Figure 10 depicts the variation of the reliability index with increased width across the seismic coefficient C. The example represented is for b=2.5 m, fc=2 MPa and t=0.3 m According to Figure 10, it is clear that as the width increases, the reliability index tends to decrease for all values of the seismic coefficient. It is also evident that a=5.2 m never reaches the TRI. In fact, across all results, this width achieves the TRI only in particular scenarios. While it performs slightly better for fc=2.5 MPa, exceeding the TRI at the thickness of 0.4 m in the very low seismicity zone (C=0.1), its performance remains limited, especially for fc=2 MPa. In this case, the TRI is met only for t= 0.5 m in a very low seismic zone and for t=0.6 m in a very low and low seismic zone (C=0.1 and C=0.13). Overall, this width proves highly restricted, requiring very low seismic demand and significantly thick walls to meet the TRI, leading the authors to recommend avoiding its use. From Figure 10, it can also be observed that a=4 m exceeds the TRI in the case of a very low seismicity zone (C=0.1). And as previously discussed for the case of a=b=4 m, and considering that, as outlined in the previous section, wall height does not significantly affect the reliability index, a=4 m exhibits similar results for b=2.5 m and b=3 m as for b=4 m, as illustrated in Figure 8. Consequently, and for the same reasons discussed for a=b=4 m, the authors do not recommend these configurations for URE walls under seismic loads.

4.6. Recommendations

Based on the previous discussion, this section summarises the general recommendations and minimum values for width, height, and thickness depending on the seismic zones for RE walls under seismic loads. These recommendations pertain to the out-of-plane bending moment for a one-story building. The recommended thickness for external URE walls in a one-story building, assuming a compressive strength of 2 MPa, is 0.15m in the case of moderate snow and wind load and 0.2 m in the case of moderate and sever snow load as well as sever snow and wind loads [33]. However, under seismic loading conditions in this study, thicknesses of 0.2 m and even 0.25 m showed poor reliability, meeting or exceeding the TRI only in restricted scenarios. This limits their applicability in structural design and highlights risks in seismic performance assessment. Therefore, Table 12 illustrates that the recommended minimum thickness recommended in this study is 0.3m, with variations depending on the seismicity zone.

This recommendation aligns with [78] and can also be considered in accordance with RPCterre [34], the American building code NMAC 14-7-4 [73], and the Nepalese standard NBC 204:1994 [80], which recommends a minimum thickness value between 0.4 m and 0.457 m (Table 6). As previously discussed, the compressive strength of 0.5 MPa demonstrates very low reliability index values compared to 2 MPa and 2.5 MPa. Consequently, the minimum recommendation of the RPCTerre [34] and the New Zealand standard NZS 4297:1998 [71] for a 0.5 MPa minimum compressive strength is inadequate.

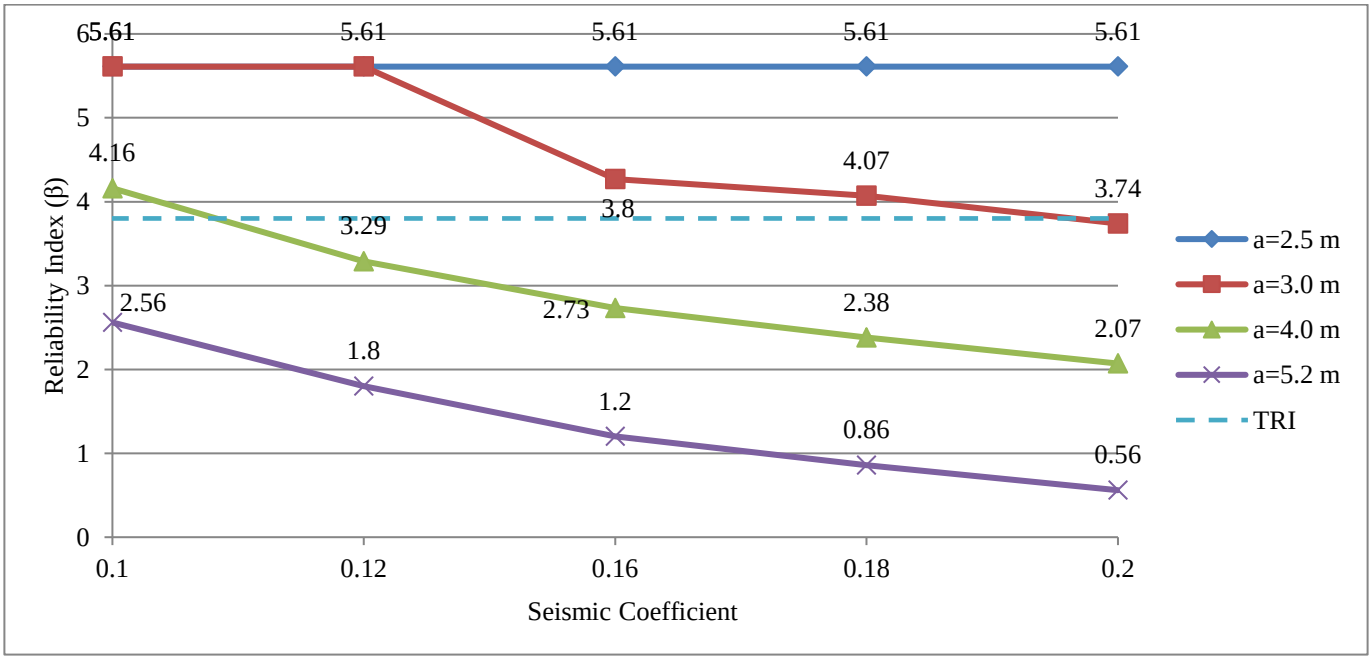

Fig. 10 Reliability index for varying width across all seismic coefficient values (t=0.3 m | b=2.5 m | fc=2 MPa)

Table 10. Failure probability and reliability index corresponding to the lowest reliability indices for all seismic coefficient values

Seismic Coefficient	Failure probability		Reliability index	
C	Pfx	Pfy	β_x	β_y
0.1	99,855	99,855	-2,978	-2,978
0.13	99,991	99,991	-3,74	-3,74
0.16	100	100	-4,611	-4,611
0.18	100	100	-4,611	-4,611
0.2	100	100	-4,611	-4,611

Table 11. Failure probability and reliability index corresponding to the highest reliability indices for all seismic coefficient values

Seismic Coefficient	Failure probability		Reliability index	
C	Pfx	Pfy	β_x	β_y
0.1	0	0	5,61	5,61
0.13	0	0	5,61	5,61
0.16	0	0	5,61	5,61
0.18	0	0	5,61	5,61
0.2	0	0	5,61	5,61

Table 12. Recommendations of minimum thickness considering wall dimensions and seismic zones

Type of material	Dimensions		Minimum Recommended Thickness (m)				
	Width a (m)	Height b (m)	C=0.1	C=0.13	C=0.16	C=0.18	C=0.2
URE	2.5	2.5	0.3	0.3	0.3	0.3	0.3
	2.5	3	0.3	0.3	0.3	0.3	0.3
	3	2.5	0.3	0.3	0.3	0.3	0.4
	3	3	0.3	0.3	0.3	0.3	0.4
	3	4	0.3	0.3	0.3	0.3	0.4

Similarly, the minimum value recommended by the Australian normative document HB 195-2002 [72] (0.4-0.6 MPa) is insufficient. In contrast, the minimum value recommended by [33] is supported by the results of this study and aligns with the American building code NMAC 14-7-4:2016 [73], which recommends a compressive strength of 2.07 MPa. Regarding the width and height of the walls, the recommended aspect ratio is $b/a \leq 1.5$. Exceeding this ratio results in differing reliability index values, introducing unpredictability that can be risky for the structure's safety. A very large bearing wall (e.g., a=5.2 m and a=4 m) is not recommended, as it only reaches the TRI in minimal configurations, requiring lower seismic zones and thicker walls. Instead, values of 2.5 and 3 m, depending on the case as illustrated in Table 12, are suitable and consistent with the existing literature. Although the excluded values do reach and exceed the TRI in specific scenarios, they may only be suitable when optimizing dimensions and compressive strength for specific cases. However, within the framework of this study, which aims to provide general recommendations rather than address specific cases, especially under seismic loading conditions, it is safer to exclude these results.

The selection of 2 MPa as the optimal minimum compressive strength is justified, as it demonstrates satisfactory performance overall, as outlined in the discussion. This choice is further supported by URE exhibiting low compressive strength, typically between 1 and 2.5 MPa, according to existing literature [13], making 2 MPa a practical and realistic benchmark. The lowest reliability indices were observed for the case of fc =0.5 MPa, t= 0.2 m, a=5.2 m and b=4 m. Conversely, the highest reliability indices corresponding to a 0% probability of failure were observed in different scenarios, as shown in the appendix. While a detailed breakdown of these scenarios is provided there, Tables 10 and 11 summarize the results for the worst and best cases, respectively. Table 12 presents the recommended minimum wall thickness values, assuming a minimum compressive strength of 2 MPa. Considering seismic loads, these final recommendations were developed based on the reliability index results for each configuration (dimensions of the URE wall and seismic coefficient), ensuring the wall can withstand out-of-plane bending moments for a one-story building. For example, in the case of a=3 m and b=2.5 m, t=0.3 m exceeds the TRI across all seismic zones except for the very high seismic zone, where the TRI is exceeded starting from t=0.4 m.

Conversely, for a=b=2.5 m, a thickness of 0.3 m is sufficient to exceed the TRI for all seismic coefficients (across all seismic zones). As shown in Table 12, a thickness of t=0.3 is identified as an adequate minimal thickness for various

configurations. However, t=0.4 m was necessary as the minimal thickness only in the case of a=3 m in a very high seismic zone (C=0.2). This demonstrates that the minimal thickness recommendation of 0.4 m in the RPCTerre [34] is accurate in some instances but represents an overdesign in most scenarios, particularly in low seismic zones and for moderately sized walls. The difference between the recommendations in this paper and those in technical documents, such as normative documents, standards and building codes, likely stems from the methodologies employed. These documents typically rely on deterministic methods, where parameters are considered in their worst-case scenarios [33]. In contrast, this study adopts a probabilistic approach, incorporating the uncertainties of various variables into the analysis. Furthermore, the divergence between this study and the only other known research that addressed the reliability analysis of RE can be attributed to the omission of seismic loads in their calculations. This omission results in lower recommended thicknesses compared to the recommendations presented here. The added value of this paper lies in its consideration of both a probabilistic framework and seismic loads, providing a more comprehensive and robust set of recommendations that address gaps in the existing literature.

5. Conclusion and Perspectives

This study focuses on URE structures' failure probability and reliability index under seismic loads subjected to out-of-plane bending moments. These were calculated as part of the structural reliability analysis framework using MCS. The limit state function was defined according to RPCTerre [34] guidelines, and random variables such as compressive strength, density, dead load, live load and roof live load were assigned their respective probability distributions. Other parameters of the limit state function, including thickness, height, and width, were treated as variables, with numerous values assessed based on the existing literature. The analysis was conducted across different seismic zones, ranging from very low seismicity to very high seismicity according to the RPCTerre [34] classification.

The results provided recommendations regarding the aspect ratio of URE walls, their width and height, and the minimum thickness required for each seismic zone. Compared to the recommendations from existing standards, guidelines and normative documents with seismic provisions, the study found some commonalities but also identified cases where recommendations were suboptimal, particularly regarding thickness in low and low seismicity zones. For compressive strength, some standards were found to recommend insufficient values given the actual mechanical properties of URE. It is crucial to note that the limit state function used to verify out-of-plane bending primarily depends on the flexural tensile strength, which, according to current research on URE [13], remains quite low.

The flexural tensile strength was replaced with its correlation to compressive strength, according to [34] guidelines, which is low compared to conventional materials. This is because, among other reasons, tensile strength is frequently overlooked in design and has not yet been thoroughly investigated [13]. Aside from being influenced by applied loads and material properties, the failure probability and reliability index also depend on the wall dimensions. The study also concludes that higher seismicity zones and greater wall widths necessitate an increase in the minimum recommended thickness. Additionally, walls exceeding 3 meters in length are only deemed acceptable in very low seismicity zones. Utilizing MCS in this study proved beneficial due to its simplicity and versatility. However, the substantial computational time required to run many iterations, such as 500,000 in this case, presents a limitation. His constraint hinders the efficient evaluation of multiple scenarios within an optimal timeframe. Therefore, employing a method that requires less computational time could be advantageous. Notably, the limit state function used was derived from the RPCTerre [34], which bases its principles of seismic justification for RE on those for unreinforced masonry. This may introduce some uncertainties in the study and results. The regulation [34] also uses a static analysis of seismic loads. Furthermore, the study employs thin plate theory as simplification; however, considering thick plate theory would be beneficial given that most cases lead to consider thick plates. It would also be valuable to explore different combinations of lateral loads. Analyzing the case of two-story RE structures would also be of significant interest, as would conducting a dynamic analysis for seismic loads to achieve greater accuracy. Future research should focus on the reliability analysis of stabilized RE, which exhibits improved flexural tensile strength. More extensive studies on RE are necessary to better characterize it, and developing a unified standardization specific to RE is crucial.

References

[1] J.E. Aubert, et al. “An Earth Block with a Compressive Strength Higher than 45MPa!” *Construction and Building Materials*, vol. 47, pp. 366-369, 2013. [CrossRef] [Google Scholar] [Publisher Link]

[2] Luisa María Gil-Martín, Manuel Alejandro Fernández-Ruiz, and Enrique Hernández-Montes, “Mechanical Characterization and Elastic Stiffness Degradation of Unstabilized Rammed Earth,” *Journal of Building Engineering*, vol. 56, 2022. [CrossRef] [Google Scholar] [Publisher Link]

[3] Mohamad M. Hallal, Salah Sadek, and Shadi S. Najjar, “Evaluation of Engineering Characteristics of Stabilized Rammed-Earth Material Sourced from Natural Fines-Rich Soil,” *Journal of Materials in Civil Engineering*, vol. 30, no. 11, 2018. [CrossRef] [Google Scholar] [Publisher Link]

[4] Lassana Bakary Traoré et al., "Experimental Assessment of Freezing-Thawing Resistance of Rammed Earth Buildings," *Construction and Building Materials*, vol. 274, 2021. [CrossRef] [Google Scholar] [Publisher Link]
[5] Matthew Hall, and Youcef Djerbib, "Rammed Earth Sample Production: Context, Recommendations and Consistency," *Construction and Building Materials*, vol. 18, no. 4, pp. 281-286, 2004. [CrossRef] [Google Scholar] [Publisher Link]
[6] Luís Mateus et al., "Mineralogical and Mechanical Characterization of Rammed Earth External Renderings of the South of Portugal ", *Construction and Building Materials*, vol. 225, pp. 1160-1169, 2019. [CrossRef] [Google Scholar] [Publisher Link]
[7] Quou Bao Bui et al., "Compression Behaviour of Non-Industrial Materials in Civil Engineering by Three Scale Experiments: The Case of Rammed Earth," *Materials and Structures*, vol. 42, pp. 1101-1116, 2009. [CrossRef] [Google Scholar] [Publisher Link]
[8] Nowamooz Hossein, and Cyrille Chazallon, "Finite Element Modelling of a Rammed Earth Wall," *Construction and Building Materials*, vol. 25, no 4, pp. 2112-2121, 2011. [CrossRef] [Google Scholar] [Publisher Link]
[9] Tiegang Zhou et al., "Investigation of Intralayer and Interlayer Shear Properties of Stabilized Rammed Earth by Direct Shear Tests," *Construction and Building Materials*, vol. 367, 2023. [CrossRef] [Google Scholar] [Publisher Link]
[10] Pierre Gerard et al., "A Unified Failure Criterion for Unstabilized Rammed Earth Materials Upon Varying Relative Humidity Conditions," *Construction and Building Materials*, vol. 95, pp. 437-447, 2015. [CrossRef] [Google Scholar] [Publisher Link]
[11] Vasilios Maniatidis, and Peter Walker, *A Review of Rammed Earth Construction*, Paper presented at DTI Project Report, Bath, 2003. [Google Scholar] [Publisher Link]
[12] T.-T. Bui et al., "Failure of Rammed Earth Walls: From Observations to Quantifications," *Construction and Building Materials*, vol. 51, pp. 295-302, 2014. [CrossRef] [Google Scholar] [Publisher Link]
[13] Fernando Ávila, Esther Puertas, and Rafael Gallego, "Characterization of the Mechanical and Physical Properties of Unstabilized Rammed Earth: A Review, *Construction and Building Materials*, vol. 270, 2021. [CrossRef] [Google Scholar] [Publisher Link]
[14] Lorenzo Miccoli, Urs Müller and Patrick Fontana, "Mechanical Behaviour of Earthen Materials: A Comparison Between Earth Block Masonry, Rammed Earth and Cob," *Construction and Building Materials*, vol. 61, pp. 327-339, 2014. [CrossRef] [Google Scholar] [Publisher Link]
[15] Fernando Ávila, Esther Puertas, and Rafael Gallego, "Characterization of the Mechanical and Physical Properties of Stabilized Rammed Earth: A Review," *Construction and Building Materials*, vol. 325, 2022. [CrossRef] [Google Scholar] [Publisher Link]
[16] Johan Vyncke, Laura Kupers, and Nicolas Denies, "Earth as Building Material - an Overview of RILEM Activities and Recent Innovations in Geotechnics," *2nd International Congress on Materials & Structural Stability (CMSS-2017)*, vol. 149, 2018. [CrossRef] [Google Scholar] [Publisher Link]
[17] Maria Idália Gomes, Teresa Diaz Gonçalves, and Paulina Faria, "Unstabilized Rammed Earth: Characterization of Material Collected from Old Constructions in South Portugal and Comparison to Normative Requirements," *International Journal of Architectural Heritage*, vol. 8, no. 2, pp. 185-212, 2014. [CrossRef] [Google Scholar] [Publisher Link]
[18] Ehsan Kianfar, and Vahab Toufigh, "Reliability and Uncertainty in Analysis of Rammed Earth Walls," *Proceedings of the 3rd World Congress on New Technologies (NewTech'17)*, Rome, Italy, 2017. [CrossRef] [Google Scholar]
[19] Juan C. Reyes et al., "Shear Behavior of Adobe and Rammed Earth Walls of Heritage Structures," *Engineering Structures*, vol. 174, pp. 526-537, 2018. [CrossRef] [Google Scholar] [Publisher Link]
[20] Luisa María Gil-Martín et al., "Mechanical Characterization and Elastic Stiffness Degradation of Unstabilized Rammed Earth," *Journal of Building Engineering*, vol. 56, 2022. [CrossRef] [Google Scholar] [Publisher Link]
[21] Alexandra H. Meek, Christopher T.S. Beckett, and Mohamed Elchalakani, "Alternative Stabilised Rammed Earth Materials Incorporating Recycled Waste and Industrial By-Products: Durability with and without Water Repellent," Construction and Building Materials, vol. 265, 2020. [CrossRef] [Google Scholar] [Publisher Link]
[22] R. Sri Bhanupratap Rathod, and B.V. Venkatarama Reddy, "Behaviour of Plain and Fibre Reinforced Cement Stabilised Rammed Earth Under Compression, Tension and Shear," *Construction and Building Materials*, vol. 344, 2022. [CrossRef] [Google Scholar] [Publisher Link]
[23] R. El Nabouch et al., "Numerical Modeling of Rammed Earth Structures: Analyses and Recommendation," *Academic Journal of Civil Engineering*, vol. 33, no. 2, pp. 72-79, 2015. [CrossRef] [Google Scholar] [Publisher Link]
[24] Thi-Loan Bu et al., "Out-of-Plane Behavior of Rammed Earth Walls Under Seismic Loading: Finite Element Simulation," *Structures*, vol. 24, pp. 191-208, 2020. [CrossRef] [Google Scholar] [Publisher Link]
[25] Ana Perić et al., "Experimental Campaigns on Mechanical Properties and Seismic Performance of Unstabilized Rammed Earth-A Literature Review," *Buildings*, vol. 11, no. 8, 2021. [CrossRef] [Google Scholar] [Publisher Link]
[26] Moein Ramezanpour, Abolfazl Eslami, and Hamid Ronagh, "Seismic Performance of Stabilised/Unstabilised Rammed Earth Walls," *Engineering Structures*, vol. 245, 2021. [CrossRef] [Google Scholar] [Publisher Link]
[27] Mehmet Emin Arslan, Mehmet Emiroğlu, and Ahmet Yalama, "Structural Behavior of Rammed Earth Walls Under Lateral Cyclic Loading: A Comparative Experimental Study," *Construction and Building Materials*, vol. 133, pp. 433-442, 2017. [CrossRef] [Google Scholar] [Publisher Link]

[28] Tiegang Zhou et al., "Seismic Performance Test of Rammed Earth Wall with Different Structural Columns" *Advances in Structural Engineering*, vol. 24, no. 1, pp. 107-118, 2021.[CrossRef] [Google Scholar] [Publisher Link]
[29] Sima Samadianfard, and Vahab Toufigh, "Stabilization Effect on the Hygrothermal Performance of Rammed Earth Materials," *Construction and Building Materials*, vol. 409, 2023. [CrossRef] [Google Scholar] [Publisher Link]
[30] Alessia Emanuela Losini et al., "Extended Hygrothermal Characterization of Unstabilized Rammed Earth for Modern Construction," *Construction and Building Materials*, vol. 409, 2023.[CrossRef] [Google Scholar] [Publisher Link]
[31] Miguel Rocha, Paulina Faria, and António Sousa Gag, "Conservation of Defensive Military Structures Built with Rammed Earth," *Buildings*, vol. 14, no. 1, 2024.[CrossRef] [Google Scholar] [Publisher Link]
[32] Wenting Chen et al., "An In-Situ Conservation Method of the Rammed Earth Sites Using a New Silica Protective Agent," *Construction and Building Materials*, vol. 452, 2024.[CrossRef] [Google Scholar] [Publisher Link]
[33] Ehsan Kianfar, and Vahab Toufigh,"Reliability Analysis of Rammed Earth Structures," *Construction and Building Materials*, vol. 127, pp. 884-895, 2016.[CrossRef] [Google Scholar] [Publisher Link]
[34] Ministry of National Territorial Planning, Urban Planning, Housing and City Policy, Ministry of National Territorial Planning, Urban Planning, Housing and City Policy, 2021. [Online]. Available: https://www.mhpv.gov.ma/fr/5121-2/
[35] Vikas Khare et al., *Chapter 6 - Reliability Assessment Model*, Tidal Energy Systems, Design, Optimization and Control, pp. 295-330, 2019. [CrossRef] [Google Scholar] [Publisher Link]
[36] Zhibao Zheng, Hongzhe Dai, and Michael Beer, "Efficient Structural Reliability Analysis Via a Weak-Intrusive Stochastic Finite Element Method," *Probabilistic Engineering Mechanics*, vol. 71, 2023. [CrossRef] [Google Scholar] [Publisher Link]
[37] Carl Rollenhagen, "Chapter 13 - Safety Culture and Safety Quality," *Radioactivity in the Environment* vol. 19, pp. 215-237, 2013. [CrossRef] [Google Scholar] [Publisher Link]
[38] Paolo Gardoni, *Risk and Reliability Analysis*, Theory and Applications Springer Series in Reliability Engineering, Springer, Cham, pp. 3 -24, 2017. [CrossRef] [Google Scholar] [Publisher Link]
[39] Peng Huang et al., "Positioning Accuracy Reliability Analysis of Industrial Robots Based on Differential Kinematics and Saddlepoint Approximation," *Mechanism and Machine Theory*, vol. 162, 2021.[CrossRef] [Google Scholar] [Publisher Link]
[40] Jinhui Wu, Yourui Tao, and Xu Han," Polynomial Chaos Expansion Approximation for Dimension-Reduction Model-Based Reliability Analysis Method and Application to Industrial Robots," *Reliability Engineering & System Safety*, vol. 234, 2023. [CrossRef] [Google Scholar] [Publisher Link]
[41] Dequan Zhang et al., "Kinematic Trajectory Accuracy Reliability Analysis for Industrial Robots Considering Intercorrelations Among Multi-Point Positioning Errors," *Reliability Engineering & System Safety*, vol. 229, 2023. [CrossRef] [Google Scholar] [Publisher Link]
[42] Yang Liu et al., "Reliability Analysis for Stall Warning Methods in an Axial Flow Compressor," *Aerospace Science and Technology*, vol. 115, 2021. [CrossRef] [Google Scholar] [Publisher Link]
[43] Hong Zhang et al., "Active Extremum Kriging-Based Multi-Level Linkage Reliability Analysis and Its Application in Aeroengine Mechanism Systems," *Aerospace Science and Technology*, vol. 131, 2022. [CrossRef] [Google Scholar] [Publisher Link]
[44] Jianqiao Liu et al., "A Study on Assigning Performance Shaping Factors of the SPAR-H Method for Adequacy Human Reliability Analysis of Nuclear Power Plants," *International Journal of Industrial Ergonomics*, vol. 81, 2021.[CrossRef] [Google Scholar] [Publisher Link]
[45] Giovanni Roma et al., "A Bayesian Framework of Inverse Uncertainty Quantification with Principal Component Analysis and Kriging for the Reliability Analysis of Passive Safety Systems," *Nuclear Engineering and Design*, vol. 379, 2021. [CrossRef] [Google Scholar] [Publisher Link]
[46] Bowen Zou et al., "Reliability Analysis and Allocation: Development of A Hierarchical Structure Modeling Platform in I&C system Software Life Cycle," *Nuclear Engineering and Design*, vol. 328, pp. 345-352, 2018. [CrossRef] [Google Scholar] [Publisher Link]
[47] Asle Natskår, and Torgeir Moan, "Structural Reliability Analysis of a Seafastening Structure for Sea Transport of Heavy Objects," *Ocean Engineering*, vol. 235, 2021. [CrossRef] [Google Scholar] [Publisher Link]
[48] Fanglong Yin et al., "Non-Probabilistic Reliability Analysis and Design Optimization for Valve-Port Plate Pair of Seawater Hydraulic Pump for Underwater Apparatus," *Ocean Engineering*, vol. 163, pp. 337-347,2018. [CrossRef] [Google Scholar] [Publisher Link]
[49] B. Zhu, H. Pei, et Q. Yang, "Reliability Analysis of Submarine Slope Considering the Spatial Variability of the Sediment Strength Using Random Fields," *Applied Ocean Research*, vol. 86, pp. 340-350, 2019. [CrossRef] [Google Scholar] [Publisher Link]
[50] Changqi Luo et al., "An Enhanced Uniform Simulation Approach Coupled with SVR for Efficient Structural Reliability Analysis," *Reliability Engineering & System Safety*, vol. 237, 2023. [CrossRef] [Google Scholar] [Publisher Link]
[51] Mariano Angelo Zanini, and Lorenzo Hofer, "Center and Characteristic Seismic Reliability as New Indexes for Accounting Uncertainties in Seismic Reliability Analysis," *Soil Dynamics and Earthquake Engineering*, vol. 123, pp. 110-123, 2019. [CrossRef] [Google Scholar] [Publisher Link]
[52] Haiyang Song, and Jian Zhang, "Structural Reliability Analysis Based on Interval Analysis Method in Statistical Energy Analysis Framework," *Mechanics Research Communications*, vol. 117, 2021. [CrossRef] [Google Scholar] [Publisher Link]

[53] Changqi Luo et al., "Hybrid Enhanced Monte Carlo Simulation Coupled with Advanced Machine Learning Approach for Accurate and Efficient Structural Reliability Analysis," *Computer Methods in Applied Mechanics and Engineering*, vol. 388, 2022. [CrossRef] [Google Scholar] [Publisher Link]

[54] Haibin Li and Xiaobo Nie, "Structural Reliability Analysis with Fuzzy Random Variables Using Error Principle," *Engineering Applications of Artificial Intelligence*, vol. 67, pp. 91-99, 2018. [CrossRef] [Google Scholar] [Publisher Link]

[55] Chao Dang et al., "Structural Reliability Analysis by Line Sampling: A Bayesian Active Learning Treatment," *Structural Safety*, vol. 104, 2023. [CrossRef] [Google Scholar] [Publisher Link]

[56] Chao Dang et al., "Parallel Adaptive Bayesian Quadrature for Rare Event Estimation," *Reliability Engineering & System Safety*, vol. 225, 2022. [CrossRef] [Google Scholar] [Publisher Link]

[57] Robert L. Harrison, "Introduction to Monte Carlo Simulation," *AIP Conference Proceedings*, vol. 1204, no. 1, pp. 17-21, 2010. [CrossRef] [Google Scholar] [Publisher Link]

[58] Ansel C. Ugural, *Plates and Shells, Theory and Analysis*, 4th ed., Boca Raton, 2017. [CrossRef] [Google Scholar] [Publisher Link]

[59] Rui Li et al., "A Unified Analytic Solution Approach to Static Bending and Free Vibration Problems of Rectangular Thin Plates," *Sciemtific Reports*, vol. 5, 2015. [CrossRef] [Google Scholar] [Publisher Link]

[60] Madhujit Mukhopadhyay, "A General Solution for Rectangular Plate Bending," *Forschung im Ingenieurwesen A*, vol. 45, pp. 111-118, 1979. [CrossRef] [Google Scholar] [Publisher Link]

[61] Ömer Civalek, "Harmonic Differential Quadrature-Finite Differences Coupled Approaches for Geometrically Nonlinear Static and Dynamic Analysis of Rectangular Plates on Elastic Foundation," *Journal of Sound and Vibration*, vol. 294, no. 4, pp. 966-980, 2006. [CrossRef] [Google Scholar] [Publisher Link]

[62] M.-H. Huang, and D.P. Thambiratnam, "Analysis of Plate Resting on Elastic Supports and Elastic Foundation by Finite Strip Method," *Computers & Structures*, vol. 79, no. 29, pp. 2547-2557, 2001. [CrossRef] [Google Scholar] [Publisher Link]

[63] H. Nguyen-Xuan et al., "A Smoothed Finite Element Method for Plate Analysis," *Computer Methods in Applied Mechanics and Engineering*, vol. 197, no. 13, pp. 1184-1203, 2008. [CrossRef] [Google Scholar] [Publisher Link]

[64] Linxiong Hong et al., "Portfolio Allocation Strategy for Active Learning Kriging-Based Structural Reliability Analysis," *Computer Methods in Applied Mechanics and Engineering*, vol. 412, 2023. [CrossRef] [Google Scholar] [Publisher Link]

[65] João B. Cardoso et al., "Structural Reliability Analysis Using Monte Carlo Simulation and Neural Networks," *Advances in Engineering Software*, vol. 39, no. 6, pp. 505-513, 2008. [CrossRef] [Google Scholar] [Publisher Link]

[66] K. Fedra, Environmental Modeling Under Uncertainty: Monte Carlo Simulation, International Institute for Applied Systems Analysis, Laxenburg, Austria, 1983. [Google Scholar] [Publisher Link]

[67] Eduard Ventsel, and Theodor Krauthammer, *Thin Plates and Shells: Theory: Analysis, and Applications*, 1st ed., Boca Raton, 2001. [CrossRef] [Google Scholar] [Publisher Link]

[68] Rudolph Szilard, *Theories and Applications of Plate Analysis: Classical, Numerical and Engineering Methods*, John Wiley & Sons, 2004. [CrossRef] [Google Scholar] [Publisher Link]

[69] David Thompson, Charles Augarde, and Juan Pablo Osorio, "A Review of Current Construction Guidelines to Inform the Design of Rammed Earth Houses in Seismically Active Zones," *Journal of Building Engineering*, vol. 54, 2022. [CrossRef] [Google Scholar] [Publisher Link]

[70] M. H. Faber, and J.D. Sørensen, "Reliability-Based Code Calibration: The JCSS Approach," *9th International Conference on Applications of Statistics and Probability in Civil Engineering - San Francisco, Californien, United States*, vol. 2, pp. 927-935, 2003. [Google Scholar] [Publisher Link]

[71] Standards New Zealand, "NZS 4297: 2020 Engineering Design of Earth Buildings," *Standards New Zealand*, 2020. [Google Scholar] [Publisher Link]

[72] Peter Walker, *The Australian Earth Building Handbook*, Standards Australia International, 2001. [Google Scholar] [Publisher Link]

[73] Issuing Agency: Construction Industries Division of The Regulation and Licensing Department, Title 14 - Housing and Construction, Chapter - 7 Building Codes General, Part 4 - New Mexico Earthen Building Materials Code, 2016. [Online]. Available : https://www.srca.nm.gov/parts/title14/14.007.0004.html

[74] Eliana Baglioni, Luisa Rovero, and U. Tonietti, *The Moroccan Drâa Valley Earthen Architecture: Pathology and Intervention Criteria*, CRC Press, 2012. [Google Scholar] [Publisher Link]

[75] BABET - Office of ParaSeismic Studies, French Standard NF P 06-001, 2024. [Online]. Available : http://babet.sarl.free.fr/surcharges.htm

[76] Vittoria Strazzeri, and Ali Karrech, "Qualitative and Quantitative Study to Assess the Use of Rammed Earth Construction Technology in Perth and the South-West of Western Australia," *Cleaner Materials*, vol. 7, 2023. [CrossRef] [Google Scholar] [Publisher Link]

[77] Ranime El-Nabouch et al., "Assessing the In-Plane Seismic Performance of Rammed Earth Walls by Using Horizontal Loading Tests," *Engineering Structures*, vol. 145, pp. 153-161, 2017. [CrossRef] [Google Scholar] [Publisher Link]

[78] Guidelines For Earthquake Resistant Design, Construction, And Retrofitting of Buildings in Afghanistan (English), United Nations Centre for Regional Development, 2003. [Online]. Available: https://uncrd.un.org/content/pub-guidelines-earthquake-resistant-design-construction-afghanistan

[79] Indian Standard: Improving Earthquake Resistance of Earthen Buildings - Guidelines, Bureau of Indian Standards, The National Standards Body of India, IS 13837: 1993, 2023. [Online]. Available: https://www.services.bis.gov.in/php/BIS_2.0/bisconnect/knowyourstandards/Indian_standards/isdetails/

[80] Guidelines For Earthquake Resistant Building Construction: Earthen Building (Eb), Nepal National Building Code NBC 204: 2015. [Online]. Available: http://www.moud.gov.np/search-page?search-field=Guidelines+for+Earthquake+Resistant+Building+Construction%3A+Earthen+Building

[81] Reza Allahvirdizadeh, Daniel V. Oliveira and, Rui A. Silva, "Numerical Modeling of the Seismic Out-Of-Plane Response of a Plain and TRM-Strengthened Rammed Earth Subassembly," *Engineering Structures*, vol. 193, pp. 43-56, 2019. [CrossRef] [Google Scholar] [Publisher Link]

[82] Quoc-Bao Bui, Ali Limam, and Tan-Trung Bui, "Dynamic Discrete Element Modelling for Seismic Assessment of Rammed Earth Walls," *Engineering Structures*, vol. 175, pp. 690-699, 2018. [CrossRef] [Google Scholar] [Publisher Link]

[83] Alric Lucas, Guy Pluvinage, and Capelle Julien, "Reliability Index of a Pipe Transporting Hydrogen Submitted to Seismic Displacement," *International Journal of Pressure Vessels and Piping*, vol. 208, 2024. [CrossRef] [Google Scholar] [Publisher Link]

[84] Mark G. Stewart, and Stephen Lawrence, "Structural Reliability of Masonry Walls in Flexure," *Masonry International*, vol. 15, no.2, pp. 48-52, 2002. [Google Scholar] [Publisher Link]

[85] Optimal Number of Trials for Monte Carlo Simulation, Valuation Research Corporation (VRC), 2017. [Online]. Available: https://www.valuationresearch.com/insights/special-report-optimal-number-trials-monte-carlo-simulation/

[86] Sheldon M. Ross, *Chapter 2 - Descriptive Statistics*, In Introduction to Probability and Statistics for Engineers and Scientists (Fourth Edition), pp. 9-53, 2009. [CrossRef] [Publisher Link]

[87] Smail Mahdi and Myrtene Cenac, "Estimating Parameters of Gumbel Distribution Using the Methods of Moments, Probability Weighted Moments and Maximum Likelihood," *Mathematics Magazine: Theory and Applications*, vol. 12, no. 1-2, pp. 151-156, 2012. [CrossRef] [Google Scholar] [Publisher Link]

[88] Numpy.random.lognormal - NumPy, 2024. [Online]. Available: https://numpy.org/doc/stable/reference/random/generated/numpy.random.lognormal.html

[89] Robert Kissell, and Jim Poserina, *Chapter 4 - Advanced Math and Statistics*, Optimal Sports Math, Statistics, and Fantasy, pp. 103-135, 2017. [CrossRef] [Publisher Link]